12-11-2013

The Osterix Reporter Mouse Identifies a Bone Marrow Skeletal Progenitor Cell Population

Sara E. Strecker
University of Connecticut, sstrecker@student.uchc.edu

The *Osterix* Reporter Mouse Identifies a Bone Marrow Skeletal Progenitor Cell Population

Sara Elaine Strecker, Ph.D.

University of Connecticut, 2013

Multipotent skeletal progenitor cells that reside in the bone marrow and contribute to the maintenance and repair of bone tissue are difficult to identify and, as a result, remain poorly understood. *Osterix* is a zinc finger transcription factor, which functions as a key regulator of bone formation. Cells of the osteoblast lineage generate bone tissue by depositing a mineralized matrix [1, 2]. *Osterix* is selectively expressed in cells of the osteoblast lineage and has an essential function in osteoblast commitment and bone formation [1, 3]. While it is generally accepted that *Osterix* is expressed in early osteogenic precursors [3, 5-7], recent studies from our lab and others have suggested that *Osterix* may be expressed at an even earlier stage of the lineage, being present in a multipotent bone marrow skeletal progenitor cell population, which can be expanded *in vitro* as a bone marrow mesenchymal stem cells (BMSCs).

To further explore the expression of *Osterix* in early bone marrow skeletal progenitor cells, we have generated *Osterix*-Cherry reporter mice. Preliminary characterization of this animal model suggests reporter expression accurately represents endogenous *Osterix* expression, being largely restricted to skeletal tissues. Additionally, FACS isolation, replating, and differentiation of *Osterix*-Cherry+ bone marrow derived stromal cells provide evidence of their skeletal multipotency, indicated by their ability to differentiate into osteoblasts, adipocytes and chondrocytes. Based on our preliminary data, we have formulated the following **hypothesis**: *Osterix* expression identifies a multipotent bone marrow skeletal progenitor cell population.

The goals of my thesis will be to: (1) characterize *Osterix* reporter expression during skeletal development and (2) characterize the bone marrow cell population expressing the *Osterix* reporter gene.

The *Osterix* Reporter Mouse Identifies a Bone Marrow Skeletal

Progenitor Cell Population

Sara Elaine Strecker

B.S., Worcester Polytechnic Institute, 2006

M.S., University of Saint Joseph, 2007

A Dissertation

Submitted in Partial Fulfillment of the

Requirement for the Degree of Doctor of Philosophy

at the

University of Connecticut

2013

APPROVAL PAGE

Doctor of Philosophy Dissertation

The *Osterix* Reporter Mouse Identifies a Bone Marrow Skeletal

Progenitor Cell Population

Presented by

Sara Elaine Strecker, B.S., M.S.

Major Advisor 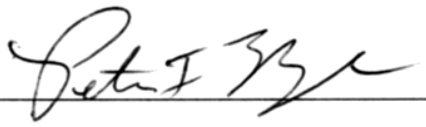

Peter F. Maye

Associate Advisor 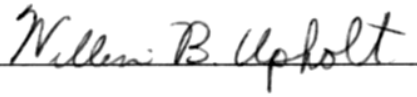

William B. Upholt

Associate Advisor 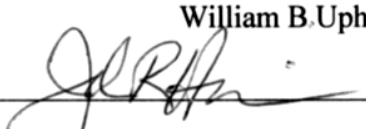

John R. Harrison

Associate Advisor 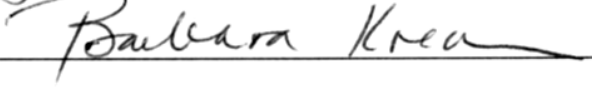

Barbara Kream

University of Connecticut

2013

ACKNOWLEDGMENTS:

I would like to thank all those who helped me along this journey, especially my colleagues: Yu Fu, Yaling Liu, and Wen Wang. A special thank you to Yaling Liu for showing me how to do everything related to cell culture and lab management as well as for being the most efficient person that I have ever met. I will be forever indebted to you. Thank you for making me feel welcome and tolerating my mistakes.

Thanks to David Rowe for the use of space and microscopes. And the people in the department, who have made these six years so special and enjoyable (alphabetically): Achint, Aja, Anu, Barb, Brya, Cheryl, Diane, Elena, Eliane, Eric, Erxia, Evan, Hrvoje, I-ping, JB, JianTao, John, Karen, Li, Liping Xiao, Liping Wang, Lyndon, Mark, Max, Nat, Neha, Paiyz, Penelope, Renata, Spenser, Thomas, Tiziana, Trushna, Vanessa, Vil, Xi, Xiaonan, Ying, Yurong, Zana, and Zhifang.

I am forever indebted to my thesis committee and all of the PIs who helped me produce my best work, Dr. Upholt, Dr. Mina, Dr. Kream, Dr. Harrison, Dr. Clark, Dr. Delany, Dr. Kalajzic, Dr. Hao, Dr. Adams, Dr. Rowe, Dr. Lichtler, Dr. Reichenberger, Dr. Goldberg, Dr. Das and my mentor, Dr. Peter Maye.

Thanks to Achint, Erin, Eilin, Julia, Matt, and Tom for keeping me mostly sane.

Mom, your support is unparalleled. Thank you for believing in me. Dad, I know you're watching from heaven – this is for you.

TABLE OF CONTENTS

LIST OF FIGURES

CHAPTER I: INTRODUCTION

THE REGENERATIVE CAPACITY OF BONE TISSUE

An increasing body of work provides evidence for the complex role of bone tissue in a variety of physiological processes. Mechanically, the skeleton provides structural support, protects delicate internal organs, allows for motion and movement, and even allows for sound conduction in the inner ear. Metabolically, bone tissue is a critical regulator of mineral homeostasis in that it is the primary site of calcium and phosphate storage which is regulated in conjunction with bone resorption and new bone deposition [6, 8-14].

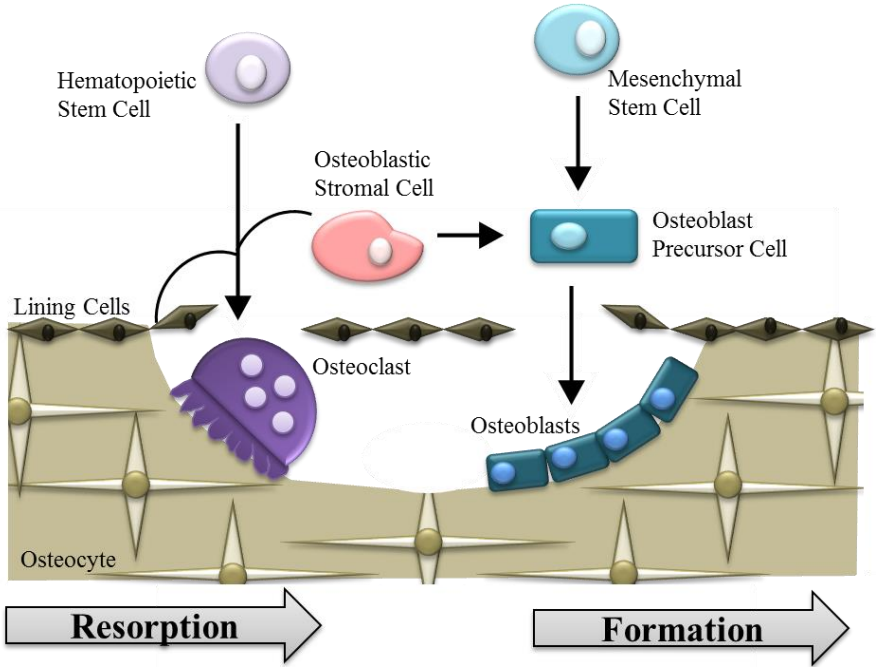

FIGURE 1 : SCHEMATIC OF BONE FORMATION AND RESORPTION

The mesenchymal stem cell gives rise to osteoblast precursors which differentiate into osteoblasts, the bone forming cells of the skeletal system. The hematopoietic stem cell gives rise to the osteoclast, which resorbs bone. **[4]**

Bone tissue also has an amazing capacity to regenerate, whether it involves the mechanisms of normal bone turnover or injury induced repair. Bone remodeling occurs throughout life. In this process, mature bone

tissue is resorbed and new bone tissue is laid down in the same place. The balance between these processes controls for the reshaping of the skeleton and allows for the repair of tissues following injury, such as overt fracture, but also in response to the micro-damage that occurs during normal activity. Remodeling the skeleton also allows for it to respond to mechanical loading. In the adult, approximately 10% of the skeleton is remodeled per year [14].

In this regard, it is generally accepted that mesenchymal stem cells provide an essential cellular source from which mature bone cells differentiate to support these regenerative processes (Fig 1) [15, 16]. However, our knowledge of mesenchymal stem cells or skeletal progenitor cells remains poorly understood. The focus of my thesis work has been on increasing our understanding of bone marrow skeletal progenitor cells.

THE DISCOVERY OF BONE MARROW SKELETAL PROGENITORS

Bone marrow stromal cells (BMSCs) were first discovered by Friedenstein in 1966 [17] and further characterized by his group as a rare cell population within the bone marrow that maintained skeletal potential [18]. Because of their skeletal potential and their accessibility through bone marrow aspiration, the application of BMSCs for therapeutic purposes has been the driving motivation to understand their biological properties. However, because of their rarity within the bone marrow, multipotent skeletal progenitors have remained a challenge to study *in vivo* and much of our understanding has been ascertained after expansion *in vitro*. In this regard, BMSCs display selective adherence to tissue culture plastic relative to most other hematopoietic cell types, retain the capacity to self-renew, support hematopoiesis, and differentiate into a variety of

connective tissue cell types, including the osteoblast, chondrocyte, and adipocyte[15, 19, 20] and are considered to be derived from a non-hematopoietic cellular component of the bone marrow stroma [21].

WHAT ARE STROMAL CELLS? (CURRENT THINKING)

BMSCs are a subpopulation of cells within the marrow and are considered to be a non-hematopoietic cellular component of the bone marrow stroma, with recent studies suggesting that the BMSC may represent a subpopulation of reticular cells [21, 22]. More recent studies have alluded to the potential identity and function of reticular cells within the bone marrow. Reticular cells are a heterogeneous perivascular cell population located adjacent to endothelial lined sinusoids within the bone marrow [23]. Reticular cells function to support different hematopoietic events, including hematopoietic stem cell retention and self-renewal and B-cell development [24, 25]. Selective isolation and characterization of CD146+ bone marrow reticular cells from human tissue has also revealed their BMSC-like properties [26, 27]. While mouse BMSCs do not express CD146, *Cxcl12*+ and *Nestin*+ murine bone marrow perivascular cells also display BMSC-like properties. Interestingly, human CD146+ reticular cells and murine *Cxcl12*+ and *Nestin*+ cells retain similar gene markers including *Cxcl12, Stem Cell Factor (SCF)*, and *Angiopoietin 1*. Surprisingly, these cells have also been shown to express *Osterix* [24, 27-29], which was previously considered to be a skeletally specific transcription factor.

Traditionally, the identity of various cell types within the bone marrow has been characterized based on cell surface profiling. Cells which express CD45 or leukocyte

common antigen, are considered to be of the hematopoietic lineage[30], cells which express CD11b are of the myeloid lineage [31], and cells which express CD31 are of the endothelial lineage [32]. The exclusion of cells which are positive for any of these three lineage markers has been used to narrow down the various cell populations within the marrow, while other markers are being sought that will define the BMSC. In mice, three specific markers have been shown to be expressed on the cell surface of putative BMSCs; these markers include Sca-1 [33], CD44 and CD29 [34]. Multiple other markers are currently being examined to try to find the one cell surface marker that defines a BMSC, as seen in the human mesenchymal stem cell / reticular cell which is positive for CD146, without luck.

ANATOMICAL ORGANIZATION OF THE BONE MARROW ENVIRONMENT

The organization of the bone marrow is a crucial clue to furthering our understanding of the various cell types which reside in this heterogeneous environment. The bone marrow is, indisputably, a complicated environment, consisting of many cell types and it is very difficult to accurately and consistently delineate different cell types within the stroma. The bone marrow itself largely consists of hematopoietic cells. With this in mind, one might think the marrow environment is largely fluid, but that is not the case. Fate mapping studies have shown that cells within the stroma do not move throughout the compartment [35, 36], but they maintain a fixed position from embryonic establishment throughout adult life [36].

Recent studies by Ding et al, have shown that different types of progenitor cells occupy physically distinct niches within the bone marrow stroma. Hematopoietic stem

cells (HSCs) occupy a perivascular niche whereas early lymphoid progenitors occupy an endosteal niche [35]. This provides more evidence that the marrow is a highly organized compartment, with a variety of cellular signals yet to be determined which are promoting and maintaining different phenotypes in a variety of cells that are in close proximity to each other. In this thesis the focus will be on osteoblasts and BMSCs which contribute to the osteoblastic lineage only, as the identity of other cells within the marrow is still being defined.

THE ORIGIN OF BONE MARROW SKELETAL STEM CELLS

ENDOCHONDRAL OSSIFICATION AND THE BONE MARROW COMPARTMENT

During embryonic development, bone tissue forms through two distinct processes termed: intramembranous ossification and endochondral ossification. Most craniofacial bones develop through intramembranous ossification where mesenchymal cells directly differentiate into osteoblasts and osteocytes [10]. Mesenchymal condensations are formed at the site of future bone development where the mesenchymal cells become osteoblasts and produce bone matrix directly. The cells which become the craniofacial skeleton are predominately derived from the cranial neural crest[37]. The axial and appendicular skeleton develop through endochondral ossification, where mesenchymal cells first condense and differentiate into chondrocytes to form a cartilaginous anlagen [6]. These skeletal cells originate from the mesoderm[37]. This cartilaginous anlagen serves as a template for bone formation as chondrocytes within the anlagen signal to the outer perichondrium providing critical signaling cues that coordinate the growth and differentiation of cartilage with bone [6]. There is generally very little marrow space in

bones which form through intramembranous ossification, whereas bones which form through endochondral ossification have a large marrow compartment. [38].

FORMATION OF THE STROMA

Formation of the stroma occurs during chondrocyte maturation and is coordinated with osteoblast differentiation. In the beginning of this process, signals secreted from hypertrophic chondrocytes trigger vascular invasion. During embryonic endochondral bone formation, factors secreted from the maturing growth plate chondrocytes initiate the expression of *Runx2* in the adjacent perichondrium. *Runx2* is a transcription factor that is considered to be at least one of the two master regulators of osteoblast differentiation. Mice deficient for *Runx2* completely lack bone tissue and gene markers of osteoblast differentiation. *Runx2* also turns on *Osterix*, another key transcription factor essential for osteoblast differentiation. Interestingly, *Osterix* knockout animals express normal levels of *Runx2*, however osteoblast differentiation remains impaired and no bone tissue forms.

Fate mapping studies have also provided evidence that perichondrial cells also migrate into the developing bone marrow compartment during this time. Embryonic cells which have been marked by *Osterix* fate mapping studies have been shown to populate the bone marrow and differentiate into osteoblasts and osteocytes. The precursors which form endochondral bone have been shown to come from a perichondrial origin. These cells migrate into the bone marrow and subsequently contribute to the bone marrow stroma [36, 39].

Previous studies have also indicated a role for *Osterix* in the osteoblast lineage, specifically in defining osteoblast commitment, but fate mapping studies have indicated the *Osterix* fate mapped embryonic precursors were not restricted to the osteoblastic lineage and instead contributed to many cell types within the bone marrow stroma. These cells included perivascular stromal cells, vascular smooth muscle, bone marrow adipocytes and perineural cells [36], indicative of the multipotency of this population. After vascular invasion occurs, much of the outer cartilage is replaced by bone as blood vessels further invade the epiphyses to form secondary ossification centers [40].

OSTERIX

Because of the important role of *Osterix* in early skeletal development, it merited further study. *Osterix* is a Cys2-His2 type DNA binding zinc finger protein belonging to the SP1 family of transcription factors. The protein itself contains three C2H2 zinc fingers along with a nuclear localization signal, enriching the location of *Osterix* to the nucleus. The mouse *Osterix* gene is found on Chromosome 15. The human homolog of the mouse *Osterix* gene maps to 12q13.13. This is a three exon gene that encodes two distinct spliceaforms. In humans, the first isoform is a 431 amino acid residue long protein isoform and the second is an amino-terminus truncated short protein isoform. Both isoforms are highly specific for osteoblasts, but some expression is seen in chondrocytes as well [41, 42].

In *Osterix* global knockout mice, the initial establishment of a cartilaginous skeletal template appears grossly normal, but osteoblast differentiation fails to occur, leading to perinatal lethality [1]. More recently, conditional knockout studies have shown

that *Osterix* is not only required for embryonic bone formation, but also for the maintenance of adult bone. Temporal inactivation of *Osterix* in postnatal and adult mice using an inducible ubiquitous Cre results in the absence of osteoblasts on the bone surface, severely altered bone structures, few mature osteoblasts and no Osteoid, leading to substantially weaker bones [3]. Interestingly, the chondrocyte specific disruption of *Osterix,* using a *Col2a1*-Cre, is also perinatal lethal. The *in vivo* patterning of endochondral bone was impaired and delayed, with expanded hypertrophic zones and significant reductions in chondrocyte specific gene markers in this model [43]. Taken together these studies indicate that *Osterix* not only has a role in osteoblast differentiation and maintenance, but is also necessary for chondrocyte differentiation [44].

USE OF FLUORESCENT REPORTER MICE TO STUDY SKELETAL PROGENITOR CELLS

In this thesis, we have used fluorescent proteins to help us study skeletal progenitor cells. Fluorescent proteins were first isolated from the jellyfish and cloned in 1992. They have since been modified to have different spectral characteristics. By 2009, over 15,000 papers have used Green Fluorescent Proteins (GFPs) or their derivatives in some form, and GFPs have been inserted into almost all laboratory species [45]. Fluorescent proteins make it much easier to track specific cells / cell types. As skeletal development is such a complex process, the use of fluorescent proteins allows for the tracing of various cells as development progresses.

In order to make the most use of fluorescent proteins we have used Bacterial Artificial Chromosomes (BACs). BACs are vectors which hold large quantities (100-

300kb) of DNA. These BACs often contain entire gene sequences as well as upstream regulatory elements. The use of BAC transgenesis to create fluorescent reporter mice involves homologous recombination and the insertion of a plasmid containing the GFP color of interest[46]. By inserting a red GFP (Cherry) upstream of the translational start site on the BAC clone and subsequent pronuclear injection, we have created a real-time reporter mouse where *Osterix* expression is marked by a Cherry GFP. By using these tools, we can compare the expression pattern of the reporter to that of endogenous *Osterix* as well as cross these *Osterix*-Cherry reporter mice with other skeletally specific lines that we have in house which utilize different spectrally distinct GFPs. This allows us to more easily break down a complex process such as endochondral ossification into its molecular parts.

Work by others and recent studies in our lab have suggested that *Osterix* expression may occur earlier than appreciated being present in multipotent BMSCs [36, 39]. Therefore, because of the struggles that the field has with identifying a multipotent BMSC, we have created and characterized an *Osterix*-Cherry Reporter mouse where these potentially important cells are marked with a cherry fluorescent protein. Early identification of a putative BMSC based on fluorescence and cell surface profiling will allow for easier isolation. Since bone marrow isolates are currently being used in various therapeutic applications, identifying the BMSC will hopefully lead to better clinical outcomes/ increased therapeutic potential.

CHAPTER II: SPECIFIC AIMS

Multipotent skeletal progenitor cells that reside in the bone marrow and contribute to the maintenance and repair of bone tissue are difficult to identify and, as a result, remain poorly understood. *Osterix* is a zinc finger transcription factor, which functions as a key regulator of bone formation. Cells of the osteoblast lineage generate bone tissue by depositing a mineralized matrix [1, 2]. *Osterix* is selectively expressed in cells of the osteoblast lineage and has an essential function in osteoblast commitment and bone formation [1, 3]. While it is generally accepted that *Osterix* is expressed in early osteogenic precursors [3, 5-7], recent studies from our lab and others have suggested that *Osterix* may be expressed at an even earlier stage of the lineage, being present in a multipotent bone marrow skeletal progenitor cell population, which can be expanded *in vitro* as a bone marrow mesenchymal stem cells (BMSCs).

To further explore the expression of *Osterix* in early bone marrow skeletal progenitor cells, we have generated *Osterix*-Cherry reporter mice. Preliminary characterization of this animal model suggests reporter expression accurately represents endogenous *Osterix* expression, being largely restricted to skeletal tissues. Additionally, FACS isolation, replating, and differentiation of *Osterix*-Cherry+ bone marrow derived stromal cells provide evidence of their skeletal multipotency, indicated by their ability to differentiate into osteoblasts, adipocytes and chondrocytes. Based on our preliminary data, we have formulated the following **hypothesis**:

Osterix expression identifies a multipotent bone marrow skeletal progenitor cell population.

AIM 1: TO CHARACTERIZE THE EXPRESSION OF *OSTERIX* REPORTER MICE DURING SKELETAL DEVELOPMENT

Temporal analysis of *Osterix* reporter expression will be carried out at embryonic, post natal and adult ages. Reporter expression will first be grossly examined macroscopically followed by a more detailed characterization in tissue section. In this analysis, *Osterix* reporter mice will also be intercrossed with previously generated osteoblast reporter mouse models to aid in its characterization. *Osterix* reporter expression will also be compared to endogenous gene expression by immunostaining on tissue sections, as well as through FACS isolation of *Osterix*+ and negative cells followed by RT-PCR.

AIM 2: TO DETERMINE IF *OSTERIX*+ BONE MARROW CELLS REPRESENT A MULTIPOTENT SKELETAL PROGENITOR CELL POPULATION.

Osterix+ bone marrow cells will be characterized to determine their identity, self-renewal and multipotent properties. Cell surface profiling and gene expression analysis will be carried out to assess the mesenchymal stem cell-like profile of *Osterix*+ bone marrow cells. Colony forming unit assays will be carried out to determine their self-renewal capacity. Also, *in vitro* differentiation assays and transplantation will be used to assess the skeletal potency of *Osterix*+ bone marrow cells.

CHAPTER III: MATERIALS AND METHODS

DNA CONSTRUCTS AND ANIMAL CARE

BAC clone RP24-362M3 was obtained from the Children's Hospital Research Institute (CHORI). The BACLinkSP linking vector was generously provided by Claire Huxley [47]. The pLD53-SC2 and pSV1.RecA recombination vectors were generously provided by Shiaoching Gong [48]. The mini lambda vector was generously provided by Donald M. Court [49]. Transgenic animals were housed in a clean barrier facility and humanely treated in accordance with University of Connecticut Health Center institutional guidelines. The *Osterix*-Cherry transgenic mouse line will become available to the research community upon acceptance of this manuscript.

CLONING HOMOLOGY ARMS INTO THE BAC LINKING VECTOR

All homology arms were amplified using Phusion DNA Polymerase (New England BioLabs) in a C1000 Thermal Cycler (BioRad). An overlapping PCR scheme was used to simultaneously clone homology arms flanking the *Osterix* gene into BACLinkSP. For this, homology arm 1 (A1) was amplified using oligos 5'Arm1OLPCR (sense) 5'-AGCTAAGGCTGGGCTTTCTTGATTTGTCTGGTGTGCATGCACCACCATGCCCAGTGACAA-3' and 3'Arm1Mlu (antisense) 5'-CTTCACGCGTCACTAACAAACGCTTCTATAATCCTTAC-3' which contained an Mlu1 site. Homology arm 2 (A2) was amplified using 5'Arm2BamH1 (sense) 5'-CTCTGGATCCGAGGGAGGAGGATCTTGACCAGCATCA-3' which contained a BamH1 site and 3' OLPCRArm2 (antisense) 5'-TTGTCACTGGGCATGGTGGTGCATGCACACCAGACAAATCAAGAAAGCCCAGCCTAGCT-3'. PCR amplified homology arms were run out on a 1% agarose gel and gel purified using a Zymoclean Gel DNA Recovery Kit (Zymo Research). The purified PCR products were eluted in 10 ul of water and diluted 1:10 in water and combined into a single tube. To promote annealing of the overlapping region, homology arms were heated to 95°C and a seven minute cool down was implemented followed by thermal cycling (95°C - 55°C - 72°C) for 25 cycles. After 25 cycles, 5' Arm2BamH1 or 3' Arm1Mlu1 primers were added to the reaction and the reaction was allowed to proceed for an additional 20 cycles. The resultant band was gel purified, restriction endonuclease digested with BamH1 and Mlu1, and cloned into the BamH1 and Mlu1 sites of pBACLinkSP using conventional cloning practices to create BACLinkSP-A1/A2.

SUBCLONING INTO BACLINKSP-A1/A2 TO CREATE BACLINKSP-*OSTERIX*

The *Red Recombinase System* was introduced into RP24-362M3 containing DH10B cells by electroporation of a mini lamda vector [49-52]. Transformants were selected on Chloramphenicol (12.5 ug/ml) plus tetracycline (10 ug/ml) LB agar plates and grown at 30°C. RP24-362M3 and mini-lambda-containing DH10B cells were made electrocompetent. Prior to harvesting cells to make them electrocompetent, bacteria were grown at 30°C and heat shocked at 42°C for 15 minutes to activate the *Red Recombinase System*.

To subclone the *Osterix* gene into BACLinkSP-A1/A2, XhoI was used to digest BACLinkSP-A1/A2 and expose the ends of homology arms 1 and 2. The linearized vector was then electroporated into RP24-362M3 and mini-lambda containing cells and selected for on LB agar plates containing Spectinomycin (50 ug/ml). Recombinants were screened by colony PCR with five separate primer pairs. Two primer pairs were designed to flank homology arms A1 and A2. Primer pairs flanking homology arm 1 were: Ost 5'Arm1Recom (sense) 5'-CTACATGATGATTCAGAACCATCTGTAACT-3' and Belo2658 (antisense) 5'-TTTGTCACAGGGTTAAGGGC-3'. Primer pairs flanking homology arm 2 were Ost 3'Arm2Recom (antisense) 5'-CAGACAAATCAAGAAAGCCCAGCCTTAGCT-3' and SP2 sense 5'-GCCCTACACAAATTGGGAGA-3'. The three remaining primer pairs amplified different regions within the *Osterix* subclone region and were used to confirm that the entire region was transferred. These three primer pairs were OstSub5'T1 (sense) 5'-TGGTCCAAGCCTGTGGACCAAGAAGCA-3' and OstSub3'T1 (antisense) 3'-

AGGAACCACCTACTGAGAGGTGGCTAT-5'; OstSub5'T2ig (sense) 5'-TCATAATGTTTCCGTGTCACCATC-3' and OstSub3'T2ig (antisense) 3'-TGCATGCGCTCTTGTGCATATGTACAT-5'; OstSub5'T3 (sense) 5'-CTTAGCAGACACATACCCGAGGATGA-3' and OstSub3'T3 (antisense) 3'-ACTGAGTCCTCTGCACCAGTTGTAAG-5'. BAC subclones positively identified by colony PCR were then further verified by Not1 and Mlu1 restriction endonuclease digestion followed by field inversion gel electrophoresis.

HOMOLOGY ARM CLONING INTO PLD53 TO CREATE PLD53-CHERRY-*OSTERIX*

A 462 base pair homology arm located just upstream of the second translational start site of *Osterix* was inserted into a pLD53.SC2-Cherry vector using standard cloning practices. The homology arm was PCR amplified using Phusion DNA polymerase using the RP24-362M3 BAC as a template. Primers Ost5'Asc1 (sense) 5'-CTCTGGCGCGCCGTAGCTGAGGATGACCTGAGGTTC-3' and Ost3'Sma1 (antisense) 3'-CTCTCCCGGGGACTGGAGCCATAGTGAGCTTCTTC-5' were used to amplify the homology arm. Amplified products were run through a PCR clean up column (Qiagen) to reduce unincorporated nucleotides, then restriction endonuclease digested with AscI and SmaI for three hours. The pLD53.SC2-Cherry vector was also restriction endonuclease digested with AscI and SmaI for three hours. After digestion, the homology arm was gel purified using a Zymoclean Gel DNA Recovery Kit (Zymo Research). The pLD53.SC2-Cherry vector was briefly treated with calf intestinal alkaline phosphatase (New England BioLabs) followed by a 1:1 phenol: chloroform extraction and precipitation. Vector and insert were mixed and ligated at room temperature for an hour using Quick Ligase (New England BioLabs) followed by electroporation into competent PIR2 cells. Bacteria were allowed to recover for a half hour before selection. Possible clones were selected for on LB plates containing ampicillin (50 ug/ml) and identified by colony PCR screening followed by diagnostic restriction endonuclease digestion with AscI and SmaI.

REPORTER GENE INSERTION TO CREATE BACLINKSP-*OSTERIX*-CHERRY

In preparation for reporter gene insertion into BACLinkSP-*Osterix*, 50 ng of pSV1.RecA was transformed into DH10B cells containing BACLinkSP-*Osterix*. After transformation, bacteria were allowed to recover for one hour without antibiotic selection followed by selection on LB agar plates containing Spectinomycin (50 ug/ml) and tetracycline (10 ug/ml) at 30°C overnight. DH10B cells containing BACLinkSP-*Osterix* and pSV1.RecA were made electrocompetent.

pLD53.SC2-Cherry-*Osterix* (1 ug) was electroporated into 50 ul of electrocompetent bacteria containing the pSV1 vector and BACLinkSP-*Osterix*. Bacteria were grown in 1 ml of LB without antibiotic selection for 1 hour at 30°C. 5 ml of LB media containing Spectinomycin (50 ug/ml), Ampicillin (50 ug/ml) and Tetracycline (10 ug/ml) were then added to the electroporated cells and the culture was grown overnight at 30°C. 200 ul of the overnight culture was spread on to an agar plate containing Spectinomycin (50 ug/ml) and Ampicillin (50 ug/ml) and grown at 42 °C overnight. Colonies were picked and screened using primers that flanked the homology arm; *Osterix*Recom (sense) 5'-GCCATCACACCAAGCCTGCTTTGTGT-3' and CherryGenotype (antisense) 5'-GCACCTTGAAGCGCATGAACTCCTTGATGA-3'. Potential BACLinkSP-*Osterix*-Cherry clones which were positively identified by PCR were then further verified by diagnostic restriction endonuclease digestion followed by field inversion gel electrophoresis.

PREPARATION OF BACLINKSP-*OSTERIX*-CHERRY FOR PRONUCLEAR INJECTION

Verified BACLinkSP-*Osterix*-Cherry clones were grown and purified from 200 ml of bacterial culture using a Maxi kit (Qiagen) with minor modifications detailed here. After alkaline lysis 2M potassium acetate was used in place of the standard 3M solution. QF buffer was heated to 65 °C for elution and the column eluate was further cleaned up with a 1:1 phenol: chloroform extraction followed by a chloroform extraction. 10 ug of the purified BACLinkSP-*Osterix*-Cherry was linearized with a SalI restriction enzyme digest and further purified on a Sepharose CL-4B column (Sigma) that had been equilibrated with injection buffer (10 mM Tris pH 7.5, 0.1 mM EDTA, 100 mM NaCl). Ten 200 ul fractions were collected and the DNA was quantified using a Nanodrop spectrophotometer (Thermo Scientific). 30 ul of each fraction was run on a pulse field gel to assess DNA quality. Pronuclear injection was carried out at the UCONN Health Center Gene Targeting and Transgenic Facility (GTTF).

HISTOLOGICAL PREPARATION OF TISSUE SAMPLES

Selected tissues were dissected and fixed in 10% Formalin buffered in PBS for 4 days at 4 °C. Hind limbs from two week old or older mice were decalcified in 15% EDTA for 4 to 7 days, depending on animal age. Tissues were then placed in 30% sucrose overnight and finally embedded in Cryomedia (Thermo Scientific). Frozen 7 um sections were obtained using a Leica Cryostat and Cryofilm type II tape transfer system (Section-Lab Co. Ltd.). Sequential tissue sections were mounted using 50% glycerol buffered in PBS for imaging.

MICROSCOPY AND IMAGING

Whole mount images of embryonic animals and kidneys were taken using a Zeiss SteREO Lumar V.12 fluorescent microscope at 9.6X and 15.4X magnification using Cherry (HQ577/20 Ex, HQ640/40 Em) and EYFP (ET500/20 Ex, ET535/30 Em) filter sets (Chroma Technologies) and photographed with an Axiocam MRm digital camera (Zeiss). Exposure times were adjusted for optimum imaging, and kept consistent throughout the experimental time course.

Tissue sections and cultures were imaged on a Zeiss Observer Z.1 microscope using Cherry (HQ577/20 Ex, HQ640/40 Em, Q595lp beam splitter), EYFP (HQ500/20 Ex, HQ 535/30 Em, Q515lp beam splitter), DAPI (AT350/50x Ex; ET460/50m Em, T400lp beam splitter) filter sets (Chroma Technologies). In some cases, the same tissue section was then stained with Mayer's hematoxylin (Poly Scientific) and photographed using an Axiocam MRc and digital camera (Zeiss) also on the Zeiss Observer Z.1 microscope.

IMMUNOSTAINING FOR ENDOGENOUS *OSTERIX*

Tissue sections were dried for 30 minutes at room temperature and then rehydrated by rinsing in PBS for 15 minutes. Sections were then permeabilized for 30 minutes in 0.1% Triton X-100 (Sigma) at room temperature. Afterwards, sections were washed twice for 10 minutes in PBS at room temperature. Non-specific staining was blocked with a 1% BSA and 5% goat serum solution (Invitrogen) in PBS for one hour. The blocking solution was removed, and the section was incubated in an *Osterix* rabbit polyclonal IgG primary antibody (Santa Cruz Biotechnologies A-13, sc-22536) at a 1:2000 dilution in 1% BSA and 1% goat serum in PBS overnight at 4 °C. Tissue sections were then washed three times at 10 minutes per wash in PBS. Tissue sections were then suspended in a solution containing the secondary antibody, goat anti-rabbit Alexa Fluor 488 (Invitrogen) at a 1:500 dilution in 1% BSA and 1% goat serum in PBS. Tissue sections were incubated with the secondary antibody at room temperature in the dark for two hours. Sections were then washed three times for ten minutes each in PBS and mounted on slides in 50% PBS-buffered glycerol for imaging.

HARVESTING AND FACS ISOLATION OF PRIMARY CELLS FROM CALVARIA AND LONG BONE

Five to seven day old mice were sacrificed and dissected to obtain their skulls and hind limbs. Soft tissues were grossly removed with a scalpel and calvaria and hind limb long bones were placed in ice cold PBS. Cells were enzymatically digested from bone tissue in a solution containing 0.625 mg/ml Collagenase P (Roche) and 0.01% Trypsin EDTA (Invitrogen) in PBS. Bone tissues were initially digested for 15 minutes in a 37°C shaker, and the supernatant from the first digestion was discarded. Three subsequent digestions were carried out for 20 minutes each. Cells from these three digestions were pooled, run through a 70 µM strainer, centrifuged at 300 x g and resuspended in 49% PBS, 49% OPTI-MEM (Gibco) and 2% FBS. Prior to FACS sorting, cells were filtered again through a 5 ml round bottom 40 µM cell strainer capped FACS tube (Falcon) and kept on ice. FACS isolation was carried out using a Vantage SE FACS sorter (BD Biosciences) at the University of Connecticut Health Center Flow Cytometry Facility. Cells were collected in 20% serum in a 1:1 mixture of OPTI-MEM (Gibco) and PBS on ice.

RNA EXTRACTION

A Nucleospin RNA/Protein Kit (Macherey-Nagel) was used to extract the RNA from sorted cell populations. In brief, cells were lysed in RA1 buffer containing B-mercaptoethanol. The resultant mixture was filtered through a column, in which the cell lysate was cleared. Ethanol was added to the filtrate and the mixture was spun through a second column, where the RNA binds to the column matrix and proteins flow through. The column membrane was desalted and then the DNA was digested, yielding a pure RNA sample in the column. The column was then washed twice with ethanol and eluted in 40 ul of RNase-free water. RNA concentrations were measured with a Nanodrop spectrophotometer (Thermo Scientific).

RNA was extracted from kidneys at different ages. Isolated kidneys were placed in Trizol (Invitrogen) and homogenized. Following the chloroform extraction, RNA was further purified through consecutive 1:1 phenol: chloroform extractions until the interface between aqueous and organic layers appeared clean. Samples were then chloroform extracted and precipitated in isopropanol. RNA pellets were washed in 75% ethanol and resuspended in DEPC treated water. RNA concentrations were measured with a Nanodrop spectrophotometer (Thermo Scientific) and RNA integrity was confirmed by gel electrophoresis.

cDNA Synthesis

RNA samples were first treated with DNAse I (Invitrogen) for 15 minutes at room temperature to remove possible genomic DNA contamination. 25 mM EDTA (Invitrogen) was added to each sample and samples were incubated at 65 °C for 10 minutes to inactive DNAse I. A master mix containing first strand buffer, random primers, DTT, and dNTPs were added to each sample. Samples were then incubated for 10 minutes at 65 °C followed by incubation on ice. RNaseOUT recombinant ribonuclease inhibitor (Invitrogen) and M-MLV reverse transcriptase (Invitrogen) were added to each tube. Samples were mixed and incubated at 37°C for 1.5 hours, and then the M-MLV was heat inactivated at 85 °C for 10 minutes.

PCR AMPLIFICATION FOR *OSTERIX* MRNA ISOFORMS

mRNA isoform specific primers were designed using Vector NTI software (Invitrogen) and the NCBI database / Primer-BLAST. $mRNA_1$ was selectively amplified using primer sets: Exon1-2 5' (sense) 5'-TTCTCTCCATCTGCCTGACTCCTT-3', Exon1-2 3' (antisense) 5'- CCATTGGTGCTTGAGAAGGGAGCTG-3'. $mRNA_2$ was selectively amplified using primer sets: Exon2 5' (sense) 5'-AGGCCACCCATTGCCAGTAA-3', Exon 2 3' (antisense) 5'-GTCATTTGCATAGCCAGAGGCTGG-3'. PCR amplification was also carried out for the Cherry reporter gene: Cherry2 5' (sense) 5'-CATCCCCGACTACTTGAAGC-3' and Cherry2 3' (antisense) 5'- CTTCAGCTTCAGCCTCTGCT-3' and GAPDH: GAPDH5' (sense) 5-CATGTTCCAGTATGACTCCACTC-3' and GAPDH3' (antisense) 5'-GGCCTCACCCCATTTGATGT-3'. PCR amplification was carried out using standard methodologies using a C1000 Thermal Cycler (BioRad).

MAINTENANCE OF ANIMALS

Osterix-Cherry mice were generated by Sara Strecker [53]. Transgenic animals were housed in a clean barrier facility and humanely treated in accordance with University of Connecticut Health Center institutional guidelines. *BSP* transgenic mice were generated by Peter Maye [54]. Mice were cared for by the Center of Animal Care (CLAC) at the University of Connecticut. Mice were monitored twice weekly by veterinary technicians. The Gene Targeting and Transgenic Facility (GTTF) injected the BAC DNA construct into the mouse. If mice showed signs of stress, they were euthanized. Adult mice were sacrificed using CO_2 inhalation and subsequent cervical dislocation, as published by CLAC. Neonatal mice were sacrificed via hypothermia followed by decapitation. The animal protocol used is 2010-605.

IMAGE ANALYSIS

The image analysis of the cortical sections was completed with the assistance of Max Villa at the University of Connecticut, Storrs, CT. Briefly, a Euclidean Distance Analysis was performed on multiple fluorescent images of cortical sections using the Image J program (NIH, [55]). The inner cortical surface was selected and a region of interest was generated. The image was converted to grayscale and a Euclidean Distance Map was generated where a white (value 0) pixel was at the center of the marrow and a black (value 255) pixel was the cortical edge. The rest of the image was coded such that the distance from the center to the edge was repented by different grayscale values. A duplicate of the original florescent image was then converted to a binary image. The distance information for the Euclidean Distance Map was combined with the binary image and a histogram was calculated, which showed the number of Cherry+ pixels as a function of distance from the endocortical surface[56, 57].

ALKALINE PHOSPHATASE STAINING

Two stock solutions were created at a concentration of 50mg/ml. Fast Blue BB 4-benzoylamino-2, 5-diethoxybenzenediazonium chloride hemi [zinc chloride] salt (Sigma) was dissolved in dimethyl formamide. NAMP 3-hydroxy-2-naphthoic acid 2, 4-dimethylanilide phosphate (Sigma) was dissolved in dimethyl sulfoxide. Both stock solutions were stored at -20°C.

Staining solutions were prepared immediately prior to use. An SB8.2 solution, containing 0.1M Tris, pH 8.0, 50mM $MgCl_2$, 100mM NaCl and 0.1% Tween20 was prepared. Stock solutions were diluted in the staining solutions separately, such that each staining solution contained 500ug/ml of either Fast Blue or NAMP. The staining solutions were mixed together in equal parts and immediately applied to the tissue section. Sections were stained for 3 minutes, rinsed in PBS and immediately cover-slipped with a 50% Glycerol, 50% PBS mixture. Staining can be visualized as blue or imaged under the Cy5 (ET620/60x Ex, ET700/75m Em, T660lpxr beam splitter) filter. *Osterix*- Cherry was imaged under the Cherry (HQ577/20 Ex, HQ640/40 Em, Q595lp beam splitter) filter.

IMMUNOSTAINING FOR CD31

Tissue sections were dried for 30 minutes at room temperature and then rehydrated by rinsing in PBS for 15 minutes. Sections were then permeabilized for 30 minutes in 0.1% Triton X-100 (Sigma) at room temperature. Afterwards, sections were washed twice for 10 minutes in PBS at room temperature. Non-specific staining was blocked with a 5% donkey serum solution in PBS for one hour. The blocking solution was removed, and the section was incubated in a CD31 (R&D Systems AF3628) at a 1:20 dilution in 1% donkey serum in PBS overnight at 4 °C. Tissue sections were then washed three times at 10 minutes per wash in PBS then suspended in a solution containing the secondary antibody, donkey anti-goat Dylight 488 (Jackson Immuno Research Labs, 705-486-147) at a 1:3500 dilution in 1% donkey serum in PBS. Tissue sections were incubated with the secondary antibody at room temperature in the dark for two hours. Sections were then washed three times for ten minutes each in PBS and mounted on slides in 50% PBS-buffered glycerol for imaging.

PREPARATION OF BONE MARROW STROMAL CELLS FOR CULTURE AND SORT

Osterix-Cherry mice were used both for cell surface profiling directly from the marrow and to derive BMSC cultures. In brief, 3-4 week old mice were sacrificed by CO_2 asphyxiation followed by cervical dislocation. Femurs and tibia were dissected from the surrounding tissues. The bones were cut through the mid-diaphysis and the bone marrow was collected through centrifugation. In brief, eppendorf tubes, each containing a filter-less column, were prepared. 200 ul of sterile cold PFE (98% PBS, 2% FBS, 2 mM EDTA) were added to the bottom of the eppendorf tube. Bones were placed, cut side down into the column and spun at high speed for 3 minutes. Single cell suspensions were prepared by gently mixing the cells with a pipette followed by filtration through a 70 μm strainer. Cells which were to be analyzed immediately were subjected to a red blood cell lysis. For the red blood cell lysis, the cells were pelleted by spinning for 5 minutes at 350g and 1 ml of Red Blood Cell Lysing Buffer (Sigma, R7757) was added to the pellet. This was gently mixed for one minute than placed on ice for three minutes. The Red Blood Cell Lysing Buffer was diluted with 10 ml of PBS and then the cells were centrifuged at 350g for 7 minute. The supernatant was decanted and the cells were prepared for further profiling.

Cells which were to be cultured did not undergo Red Blood Cell Lysis and were plated at a density of 1.2×10^6 cells/cm^2 in αMEM culture medium containing 100 U/ml penicillin, 100 μg/ml streptomycin and 10% FCS (Hyclone). At day 4, the media was changed. On day 5, the cells were sorted and processed. In some cases, cells were cultured for a 21 day time period. In these cases, cells were grown in αMEM culture

medium containing 100 U/ml penicillin, 100 μg/ml streptomycin and 10% FCS (Hyclone) for 7 days, with the media being changed on Day 4 and Day 7. On Day 7, the media was supplemented with 50 μg/ml ascorbic acid and 8 mM 2-glycerol phosphate and changed every two days until Day 21.

FACS ANALYSIS

Cultured cells were washed twice with cold PBS then digested using a sterile filtered mixture of 0.1% Collagenase P (Roche), 0.1% Hyaluronidase (Sigma), 2% FBS (Hyclone), 49% OPTI-MEM (Gibco) and 49% PBS (Gibco). Cells were digested for 10 minutes at 37°C, scraped, then digested for an additional 5 minutes at 37°C. The digestion was stopped using an equal amount of media containing 2% FBS, 49% PBS and 49% OPTI-MEM. At this point, cultured cells and cells from the marrow were treated in the same manner. Cells were counted and then centrifuged at 300g for 10 minutes. Up to 10^7 nucleated cells were resuspended in 100 ul FACS staining buffer (PBS, 0.5% BSA, 2 mM EDTA, pH 7.2). 10 ul of the appropriate antibody was then added to the cell suspension. This was mixed well and incubated for 10 minutes in the dark at 4 °C. Next the cells were washed by the addition of 1-2 ml of buffer and subsequent centrifugation at 300 g for 10 minutes. The supernatant was aspirated and the cells were resuspended in 500 ul of staining buffer for FACS analysis.

Antibodies used were all conjugated to APC in order to be spectrally distinct from the Cherry and included CD11b (Miltenyi, 130-091-241), CD31 (Miltenyi, 130-097-420), CD45 (Miltenyi, 130-091-811), CD44 (Miltenyi, 130-096-836), CD140b (Miltenyi, 130-096-270) CD105 (Miltenyi, 130-092-930), Anti-Sca1 (Miltenyi, 130-093-223), CD29 (Miltenyi, 130-096-356) and CD90.2 (Miltenyi, 130-091-790). Cells were analyzed on the FACS LSRII (BD) using the Red 649 nm Laser (670/30) and the YS 561 nm Laser (610/20, 600LP). The Blue 488 nm Laser (530/30, 505LP) was sometimes used to gate out auto-fluorescent cells.

FACS SORTING

Cells from the bone marrow were sorted using the 70 um nozzle on the FACS Aria (BD). Cells which had been cultured were also sorted on the FACS Aria, however the 130 um nozzle was used. Cells were sorted for mCherry using the Green Laser (610/20, 600LP), APC using the Red Laser (660/20) and GFP using the Blue Laser (530/30, 505LP). Cells were originally sorted into media containing 20% FBS (Hyclone), 40% PBS (Gibco) and 40% OPTI-MEM (Gibco). However, our current research is suggesting that the cells remain viable for a longer period of time if they are sorted into media containing 2% FBS (Hyclone), 49% PBS (Gibco) and 49% OPTI-MEM (Gibco), therefore, sorts conducted in Chapter I were sorted into 20% serum containing media and sorts conducted in Chapter II were sorted into media containing 2% serum.

DIFFERENTIATION OF ISOLATED CELL POPULATIONS

After FACS, isolated cell populations were initially plated as a spot with ~ 2×10^4 cells in 10 μl of medium (αMEM culture medium containing 100 U/ml Penicillin, 100 μg/ml streptomycin and 10% FCS (Hyclone)) for osteogenic and adipogenic differentiation. 2×10^6 cells were plated in a 10 ul spot for chondrogenic differentiation. After 2 hours, αMEM culture medium containing 100 U/ml penicillin, 100 μg/ml streptomycin and 10% FCS (Hyclone) was added to the spot cultures. Osteogenic differentiation was induced with the addition of 50 μg/ml ascorbic acid, and 8 mM 2-glycerol phosphate to the culture media on Day 1 and cells were maintained in differentiation media for 8 days. Adipogenic differentiation was induced with the addition of 1.0 uM insulin and 0.5 uM Rosiglitizone to the culture media on Day 1 and cells were maintained in differentiation media for 8 days. Chondrogenic differentiation was induced on Day 1. Cells were cultured in high glucose DMEM which was supplemented with ITS+1, 50 μg/ml ascorbic acid, 100 μg/ml sodium pyruvate, 0.1 uM dexamethasone, 100 U/ml penicillin, 100 μg/ml streptomycin, 40 μg/ml L-proline and 10 ng/ml TGF-B3.

HISTOLOGICAL EVALUATION OF ISOLATED CELL POPULATIONS

Osteogenesis was assessed through von Kossa staining. Cultures were washed with PBS then fixed in 10% formalin for 10–15 min. Cultures were next rinsed with water and a 5% silver nitrate solution was added. Cross-linking to evaluate the amount of phosphate deposition was performed for 2 cycles at 1200 µjoules × 100 in a UV Stratalinker (Stratagene, La Jolla, CA). Mineralized nodules appear as dark spots. Cultures counterstained with Mayer's Hematoxylin.

Adipogenesis was assessed through Oil Red O staining. In brief, cultures were washed in PBS and fixed for 10 minutes in 10% formalin. After fixation, cultures were washed with water and air dried. The 0.5% stock Oil Red O solution was diluted to 0.3%, filtered through Whatman #1 filter paper, and then added to the dry cultures. This was incubated for 1 hour at room temperature and the stain was aspirated. Cultures were washed twice with water and counterstained with Mayer's Hematoxylin.

Chondrogenesis was assessed through Alcian Blue staining. Cultures were rinsed with PBS then fixed with 10% formalin for 10 minutes. Cultures were then briefly rinsed with a solution of 3% glacial acetic acid (pH 1.0). Alcian blue staining was carried out overnight using a 1% Alcian Blue solution (pH 1.0). Excess staining was removed through a wash in 3% glacial acetic (pH 1.0) and then two washes with 3% glacial acetic acid (pH 2.5).

CHAPTER IV: GENERATION AND CHARACTERIZATION OF *OSTERIX*-CHERRY REPORTER MICE

ABSTRACT

Osterix is a zinc finger containing transcription factor and functions as a key regulator of osteoblast differentiation. To better understand the temporal and spatial expression of *Osterix* during embryonic development and in the adult skeleton, we generated *Osterix*-Cherry reporter mice. Bacterial recombination techniques were employed to engineer a transgenic construct, which consisted of a ~39kb DNA fragment encompassing the *Osterix/Sp7* gene, but excluding adjacent gene sequences. *Osterix* reporter expression was characterized at embryonic, neonatal, and adult ages both by itself and in the context of a cross with *Bone Sialoprotein* (*BSP*)-Topaz reporter mice. Relative to *Osterix*, *BSP* is a more mature marker of osteoblast differentiation. In agreement with osteoblast lineage maturation, *Osterix* reporter expression preceded *BSP* reporter expression during embryonic development and spatially appeared in a much broader cell population. Strong *Osterix* reporter expression was observed in mature osteoblasts and osteocytes. However, weaker *Osterix*-Cherry+ cells were also observed in the bone marrow, possibly identifying an early osteoprogenitor cell population. Evaluation of *Osterix* reporter expression in male femur tissue sections from 10 days to 12 weeks of age revealed persistent expression in cells of the osteoblast lineage and a surprising increase in maturing chondrocytes of the growth plate. Also, *Osterix* reporter expression was transiently detected in the kidney after birth.

INTRODUCTION

Bone development occurs through two different processes termed intramembranous ossification and endochondral ossification [6, 58-60]. Most bones of the craniofacial skeleton develop through intramembranous ossification, where mesenchymal cells directly differentiate into cells of the osteoblast lineage. However, in the axial and appendicular skeleton, all bones develop through endochondral ossification, in which mesenchymal cells first condense and differentiate into chondrocytes that form cartilaginous anlagen. The cartilaginous anlagen serves as a physical template for bone formation and chondrocytes within the anlagen signal to the outer perichondrium, providing critical signaling cues that coordinate the colonization/replacement of cartilage by bone.

Genetic studies in mice have revealed that *Osterix* is a key transcriptional regulator of osteoblast differentiation and, more recently, of chondrocyte maturation. *Osterix* is a Cys2-His2 type zinc finger protein that binds DNA and belongs to the *SP1* family of transcription factors [1]. In *Osterix* global knockout mice, the initial establishment of a cartilaginous skeleton appears grossly normal, but osteoblast differentiation fails to occur, leading to perinatal lethality [1]. Global inactivation of floxed *Osterix* at postnatal and adult ages using *Cag*-CreER mice resulted in loss of osteoblasts on the bone surface and progressive deterioration of bone tissue, revealing that *Osterix* continues to have an essential role in maintaining bone tissue at adult ages [3]. Selective deletion of *Osterix* with *Col2a1*-Cre has also revealed an important role for *Osterix* in chondrocyte maturation. Loss of *Osterix* in chondrocytes resulted in an

expanded hypertrophic zone that failed to completely mature, resulting in a significant delay and reduction in vascular invasion and bone remodeling by osteoclasts [43].

RESULTS

To increase our understanding of *Osterix* gene expression at embryonic and adult ages, we generated *Osterix*-Cherry reporter mice. The *Osterix* gene is located in a relatively gene rich area on mouse chromosome 15. Therefore, in designing the transgene, we decided to separate *Osterix* from these neighboring genes by subcloning a 39kb DNA fragment containing the *Osterix* gene using a bacterial recombination approach (Fig.2A). This subcloned DNA fragment includes 24457 bp of sequence upstream of the first translational start site and ends 6920 bp downstream of the stop codon. To verify the isolated region's identity, Not1 and Mlu1 restriction endonuclease digests were carried out. Two predicted bands, one at approximately 22 kb and the second at 25 kb were observed, thereby identifying three positive clones (Fig. 2B). Work by others [2, 41] and our own alignment of mRNA transcripts deposited into the NCBI database have shown that *Osterix* transcription yields two alternatively spliced mRNAs. $mRNA_1$ encodes for a slightly larger 428 amino acid isoform whose translation starts in exon 1, while $mRNA_2$ encodes for a shorter 410 amino acid isoform whose translation starts in exon 2 (Fig. 2C). The second downstream translation start site is in frame with the upstream translation start site. Therefore, we decided to insert a Cherry fluorescent protein reporter just upstream of the second translation start site in order to detect both *Osterix* isoforms (Fig.2C, red arrow head). To confirm the targeted insertion of the Cherry reporter, colony PCR was carried out using primers that flank the 462 bp homology box (Fig. 2D). Pronuclear injection of the DNA construct resulted in generation of two different founder lines. Gross evaluation of reporter gene expression from F1 and F2 offspring from both founder lines showed identical expression patterns

(data not shown). Thereafter, we have primarily focused on one founder line and present a more detailed characterization of its reporter gene expression here.

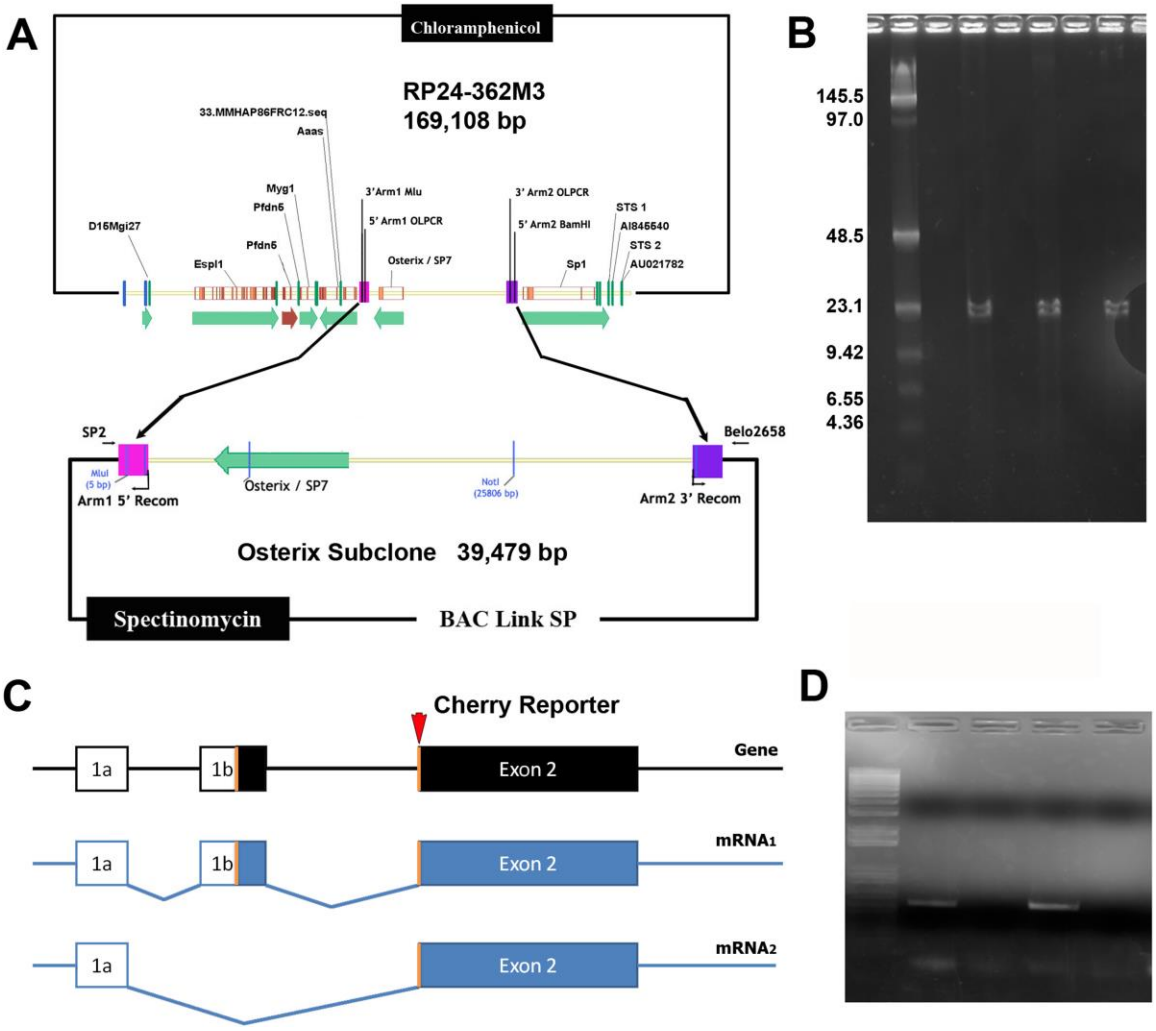

FIGURE 2: ASSEMBLY OF *OSTERIX*-CHERRY TRANSGENE

(a) A 39 kb region containing the *Osterix* gene and flanking DNA sequences was subcloned from BAC clone RP24-362M3 into BACLink-SP. **(b)** Potential subclones were confirmed by a diagnostic restriction endonuclease digestion with Mlu1 and Not1, which showed two DNA fragments at 25 and 22 kb. **(c)** Diagram of the *Osterix* gene (black) mapped with two alternatively spliced mRNA transcripts (blue). Two alternative translational start sites also exist. The first translational start site is located in exon 1b and results in the creation of a long protein isoform (mRNA1) consisting of 428 amino acids. The second translational start site is located near the beginning of exon 2, is in frame with the upstream translational start site, and results in the creation of a shorter protein isoform (mRNA2) consisting 410 amino acids. The Cherry reporter was inserted via homologous recombination just upstream of the second translational start site of the *Osterix* gene (red arrow) allowing us to detect both transcriptional isoforms. **(d)** Gel image of colony PCR screening to identify clones where the Cherry reporter was appropriately inserted into the construct. Two positive clones are shown.

To aid in the characterization of *Osterix*-Cherry mice, we compared their reporter expression to that of a *Bone Sialoprotein* (*BSP*)-Topaz reporter mouse line [54]. During

osteoblast differentiation, *Osterix* expression precedes *BSP* and is required for *BSP* expression [61]. The *BSP* –Topaz reporter line utilizes a fluorescent protein that is spectrally distinct from Cherry fluorescent protein, allowing us to simultaneously image both reporters and visualize immature and mature osteoblast cell types. *Osterix*-Cherry reporter expression (red) was characterized relative to *BSP*-Topaz reporter expression (green) from days E13.5 to E17.5 of embryonic development. Congruent with skeletal development occurring asynchronously in an anterior to posterior progression, *Osterix* reporter expression was first detected at E13.5 in craniofacial bones and weakly in the fore limbs (Fig. 3A). *BSP* reporter expression was also detected at E13.5 (Fig. 3B); however the domains of *Osterix* reporter expression were noticeably broader than those of the *BSP* reporter (Fig. 3 Compare A to B, and C). At E15.5, *Osterix* reporter expression increased relative to E13.5 and now can be detected in the ribs and hind limbs (Fig. 3D). Levels of *BSP* reporter expression have also increased from E13.5 to E15.5 and globally appear in the same regions as *Osterix* (Fig.3 E and F). The progression of osteoblast maturation can be appreciated at higher magnification in the frontal and parietal bones of the skull (Fig.3 G-I) and the radius, ulna, and humerus of the fore limb (Fig.3 J-K). Again, the domains of *Osterix* reporter expression are broader than those controlled by *BSP* and show the transition from osteoprogenitor to a maturing osteoblast. Both *Osterix* and *BSP* reporters at this age are osteoblast specific and do not appear in other connective tissue cell types such as the sutures of the skull (Fig.3 G-I) or in joints of the appendicular skeleton (Fig.3 J-L). At E17.5 the expression levels of *Osterix* and *BSP*

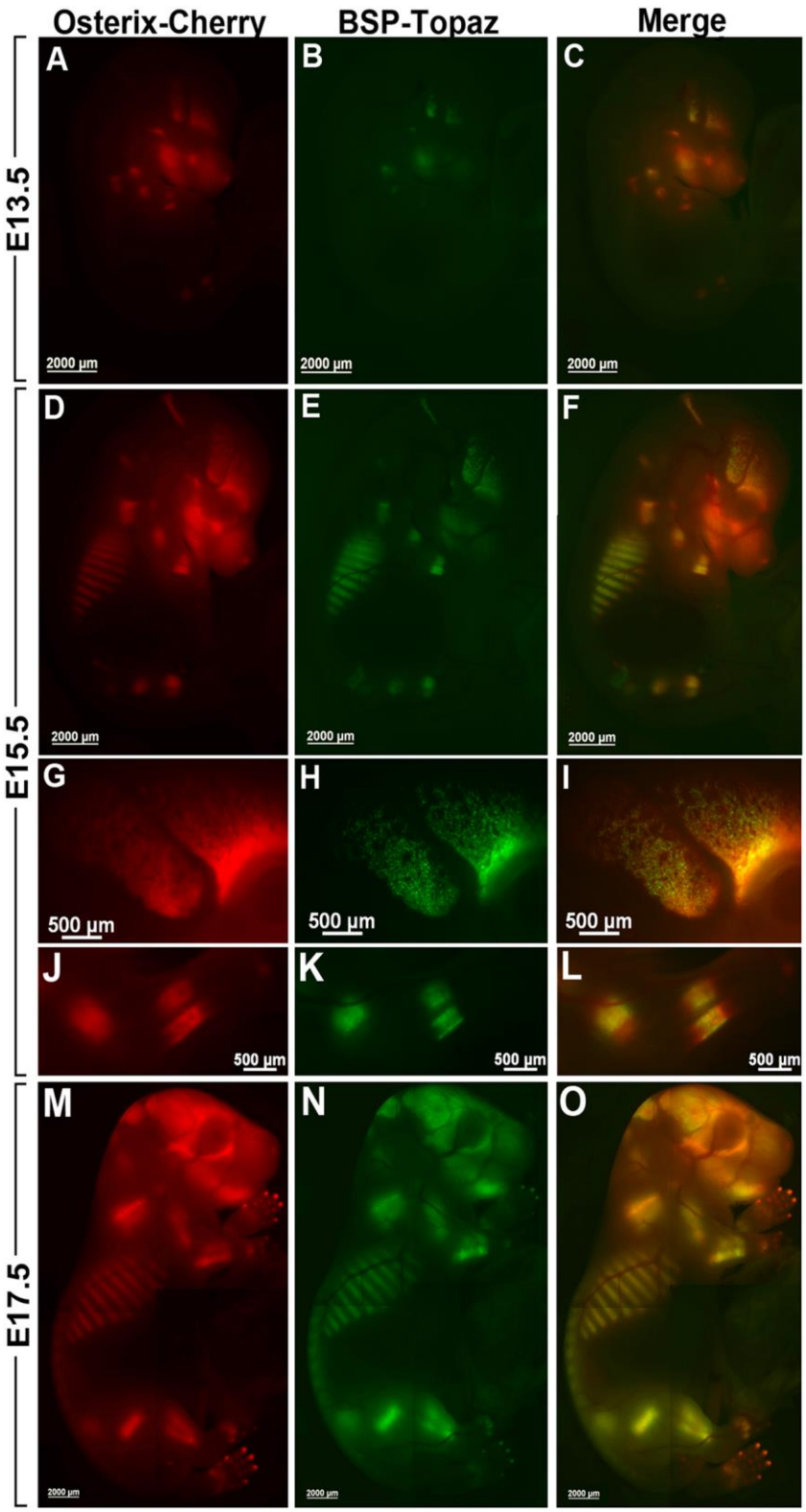

FIGURE 3: COMPARISON OF OSTERIX REPORTER EXPRESSION TO BONE SIALOPROTEIN

(a–o) Whole embryo imaging of reporter gene expression from E13.5–E17. **(a ,d, g, j, m)** Osterix-Cherry reporter expression (red). **(b, e, h, k, n)** Bone Sialoprotein – Topaz reporter expression (green). **(c, f, i, l, o)** Merge of Osterix and Bone Sialoprotein reporter expression yellow indicates where the signals overlap). **(a–c)** Comparison of Osterix and Bone Sialoprotein reporter expression at E13.5 **(a)** Osterix reporter expression is first detected at E13.5 in the developing craniofacial bones and in the fore limbs. Very weak Osterix reporter expression is detected in the developing hind limbs. **(b)** The onset of Bone Sialoprotein reporter expression is also detected at E13.5. **(c)** The merged image confirms the overlap between both osteoblast reporter models; however, the Osterix reporter is expressed in a considerably broader cell population than the Bone Sialoprotein reporter. **(d–i)** Comparison of Osterix and Bone Sialoprotein reporter expression at E15.5. **(d)** Levels of Osterix reporter expression have increased relative to E13.5 and are now easily detected in the hind limbs and ribs in addition to the bones of the craniofacial skeleton and fore limb. **(e)** Levels of Bone Sialoprotein reporter expression have also increased since E13.5 and appear in the same skeletal elements as the Osterix reporter as shown in the merged image **(f)**. While both reporter genes are expressed in the same skeletal elements, the broader cellular expression of the Osterix reporter relative to the Bone Sialoprotein reporter is apparent and appreciated at higher magnification in the skull **(g–i)** and fore limb **(j–l)**. **(m–o)** Osterix and Bone Sialoprotein reporter expression at E17.5. Osterix reporter expression is now detected in the vertebrae and developing digits, whereas the Bone Sialoprotein reporter is seen in the spine, but has not yet appeared in the metatarsals.

reporters continued to increase (Fig.3 M-O). *Osterix* and *BSP* reporters are now detected in the vertebrae and pelvic girdle. Also, as limb development progresses in a proximal to

distal fashion, *Osterix* reporter expression is detected in the digits of the paws (Fig.3 M-O).

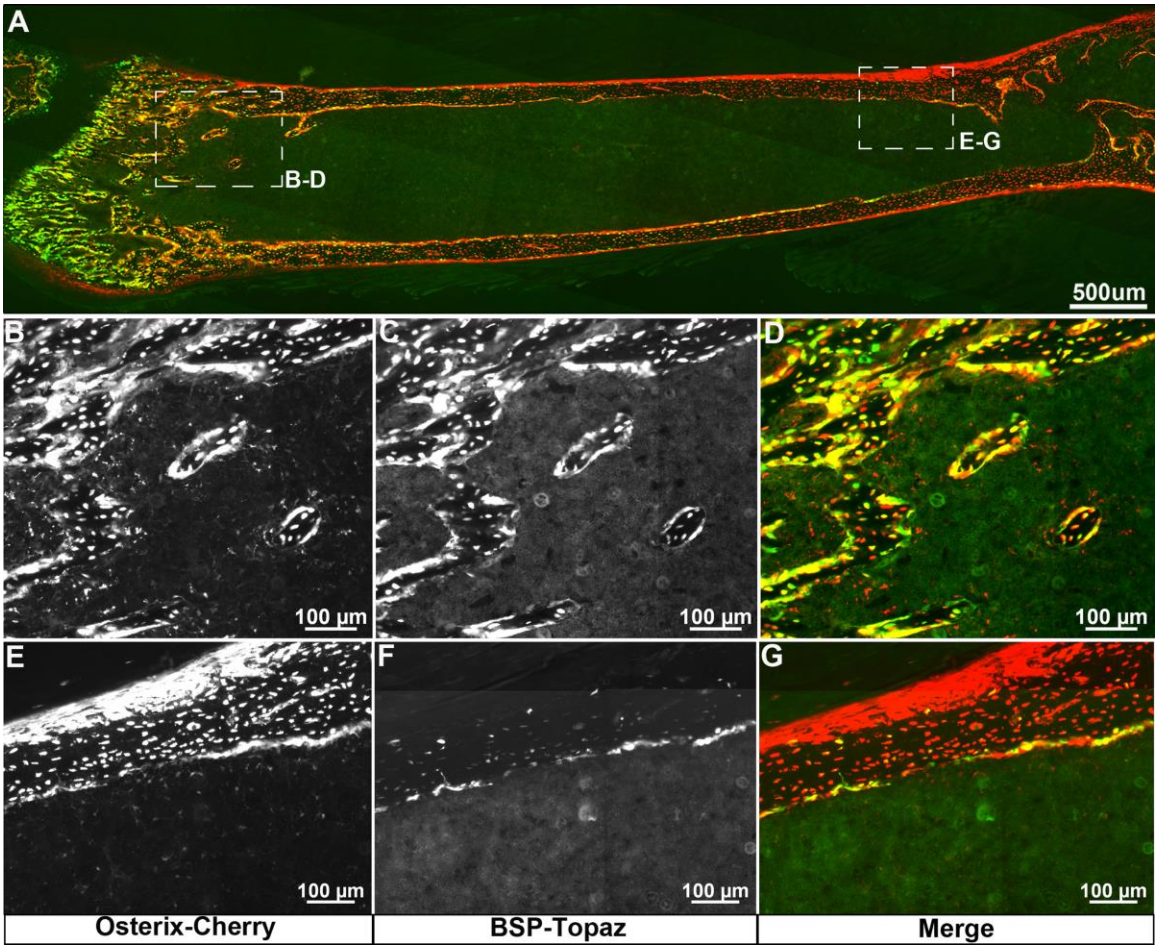

FIGURE 4: COMPARISON OF *OSTERIX* REPORTER EXPRESSION TO BONE SIALOPROTEIN REPORTER EXPRESSION IN A TISSUE SECTION THROUGH A 3-WEEK-OLD FEMUR.

(a) Merged image of *Osterix*-Cherry (red) and Bone Sialoprotein-Topaz (green) reporter expression. Global visualization of reporter expression revealed that the *Osterix* reporter is intensely and uniformly expressed in osteoblasts within the trabecular and cortical bone regions. In contrast, Bone Sialoprotein reporter expression was not as uniformly expressed as the *Osterix* reporter and appeared at higher levels within the trabecular bone region and at lower levels in cortical bone. This is better appreciated at higher magnification [regions of interest are denoted by dashed boxes **(b–d)** and **(e–g)**]. **(b and e)** *Osterix* reporter expression was strongly expressed in osteoblasts and osteocytes within trabecular bone **(b)** and cortical bone **(e)**. Low *Osterix* reporter expression was also detected in a cell population present in the bone marrow, but in proximity to trabecular and cortical bone surfaces. **(c and f)** Bone Sialoprotein reporter expression was strongly detected in osteoblasts and osteocytes in the trabecular bone region **(c)**, but was expressed at lower levels and appeared with less frequency in osteoblasts and osteocytes present in cortical bone **(f)**. Unlike the *Osterix* reporter, the Bone Sialoprotein reporter was not detected in any cells within the bone marrow. **(d and g)** Merged images reveal the expression of both reporters relative to each other in the trabecular and cortical bone regions.

Characterization of *Osterix*-Cherry reporter expression was also compared to *BSP*-Topaz reporter expression in tissue sections through a 3 week old femur (Fig. 4). The whole femur was imaged for both reporters (Fig. 4A) and areas of trabecular bone (Fig. 4B-D)

and cortical bone (Fig. 4E-G) are shown at higher magnification. *Osterix* reporter expression was robustly and broadly expressed in cells of the osteoblast lineage (Fig. 4A). Strong *Osterix* reporter expression is present in mature osteoblasts lining trabecular and cortical bone surfaces and osteocytes embedded within bone tissue (Fig. 4, A, B, and E). In contrast, *BSP* reporter expression is not nearly as uniform as the *Osterix* reporter. High levels of *BSP* reporter expression were detected just below the growth plate within the trabecular bone region (Fig. 4 A and C), but gradually decreased as the distance from the growth plate increased, with lower *BSP* reporter expression being present in osteoblasts on the cortical bone surfaces in the mid-diaphysis region (Fig. 4 compare C to F). Also, the frequency of *BSP*+ cells was higher on the endosteal bone surfaces relative to the outer periosteum (Fig. 4 F and not shown). In addition to the *Osterix* reporter being strongly expressed in osteoblasts and osteocytes, we also noted the detection of a bone marrow cell population situated in proximity to bone surfaces that retained lower *Osterix* reporter expression (Fig. 4 B and E). The *BSP* reporter was not detected in this bone marrow cell population (Fig. 4 C and F), suggesting this may be a very early osteoprogenitor cell type.

Loss of function studies at postnatal to adult ages have indicated that *Osterix* continues to play an essential role in the maintenance of bone tissue [7, 44, 62, 63]. Consistent with these studies, the evaluation of *Osterix* reporter expression in male femurs at increasing ages (10 days, 3 weeks, 8 weeks, and 12 weeks) suggests that *Osterix* expression persists in cells of the osteoblast lineage into adulthood (Fig. 5). Interestingly, in this temporal analysis we also detected an increase in *Osterix* reporter expression in maturing chondrocytes of the growth plate. In three week old animals,

FIGURE 5: STRONG AND PERSISTENT *OSTERIX* REPORTER EXPRESSION IN BONE CELLS WITH AGING.

Osterix reporter expression and corresponding hematoxylin stained tissue sections at postnatal day 10 **(a, a')** 3 weeks **(b, b')**, 8 weeks **(c, c')**, and 12 weeks of age **(d, d')**. *Osterix* reporter expression persisted with aging in osteoblasts and osteocytes present in the trabecular and cortical bone regions. Fixed exposure times were used and all femurs were taken from male mice.

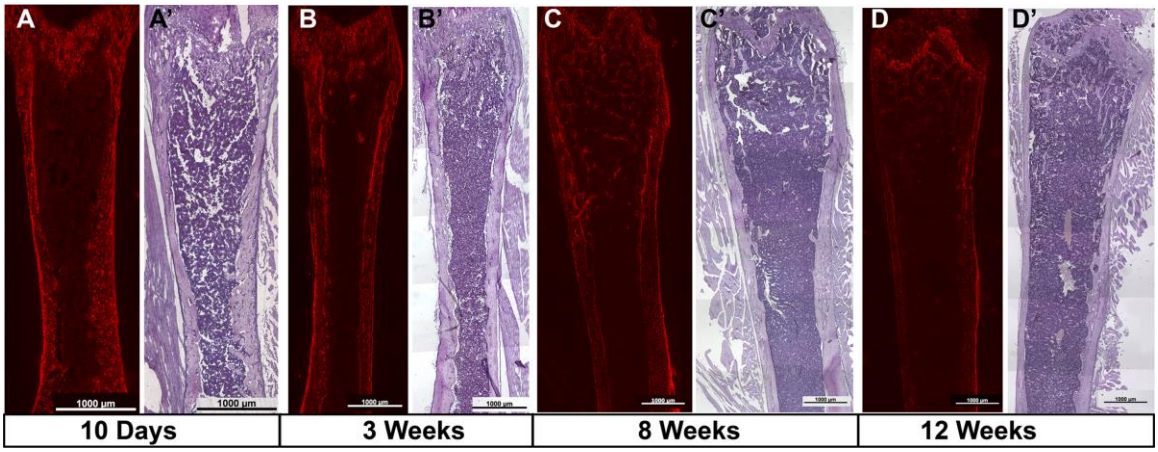

expression of the *Osterix* reporter was very weak in the growth plate relative to the level of reporter gene expression detected in the bone cells (Fig. 6A). However, by 8 weeks of age, *Osterix* reporter expression was easily detected in maturing chondrocytes (Fig. 6B) and at twelve weeks of age, the area of the growth plate retaining *Osterix* reporter expression was arguably the highest expressing region within the bone (Fig. 6C).

FIGURE 6: INCREASE IN OSTERIX REPORTER EXPRESSION IN GROWTH PLATE CHONDROCYTES WITH AGING

(a–c) A fixed exposure time was used to compare the fluorescence intensity of Osterix reporter expression in growth plate chondrocytes at 3 weeks **(a)**, 8 weeks **(b)**, and 12 weeks of age **(c)**. While the Osterix reporter can be detected in growth plate chondrocytes in 3-week-old mice **(a)**, there is a substantial increase in reporter expression detected in 8-week-old mice **(b)**, which continues to increase with age as shown in 12-week-old mice **(c)**.

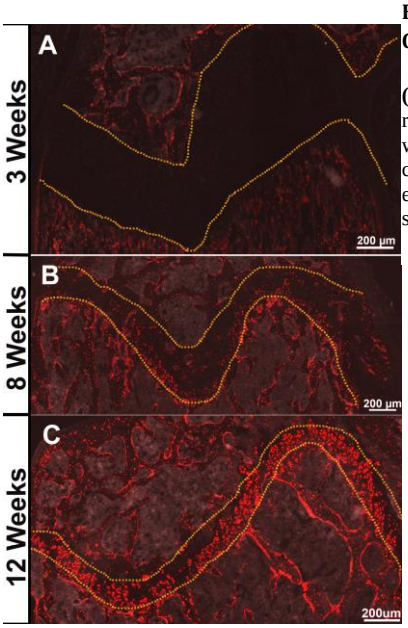

To determine if expression of the *Osterix* reporter represents endogenous *Osterix* gene expression, we compared *Osterix* reporter expression to endogenous levels of *Osterix* protein by immunostaining. Immunostaining for *Osterix* was initially carried out directly on bone tissue sections derived from *Osterix* transgenic mice. However, we soon

learned that the polyclonal antibody that worked extremely well in our hands recognized our reporter gene. The reason for this is that we cloned into the second exon, just upstream of the second translational start site, in order to detect both transcriptional isoforms. In doing so, transcription and translation of $mRNA_1$-Cherry results in the creation of a small protein fusion in which the first 17 amino acids of *Osterix* are present on the N-terminal of the Cherry reporter. Correspondence with Santa Cruz Biotechnologies confirmed that the

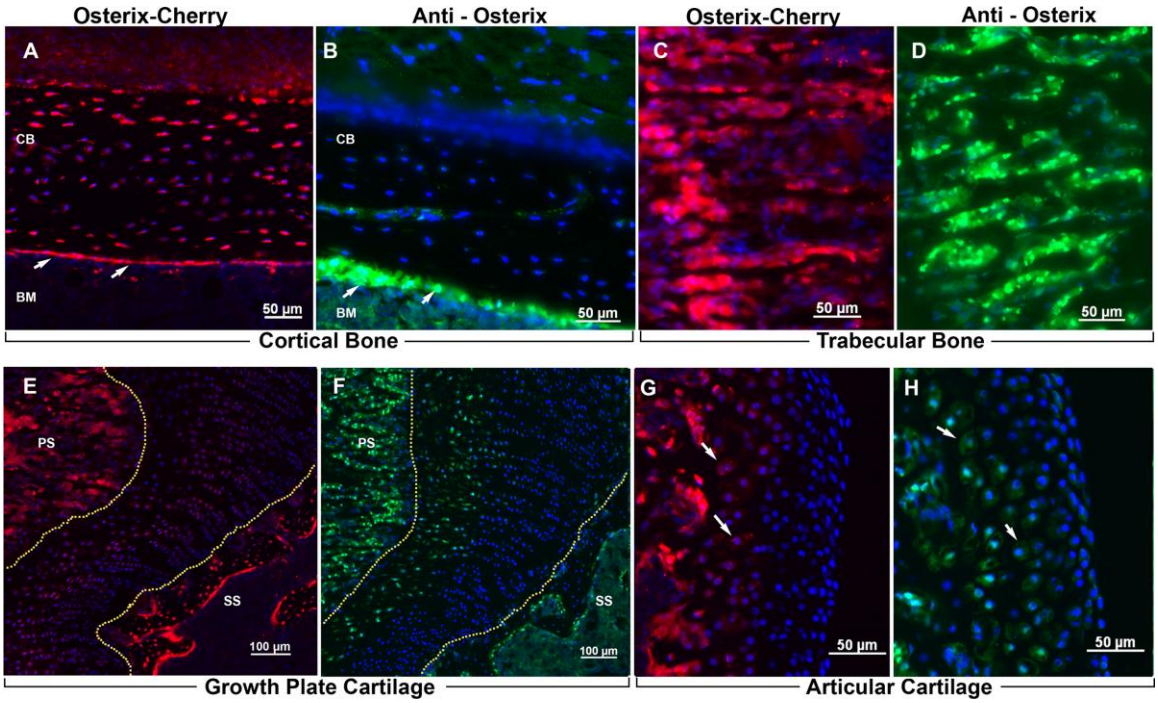

FIGURE 7: COMPARISON OF *OSTERIX* REPORTER EXPRESSION TO IMMUNOSTAINING FOR *OSTERIX* PROTEIN

Osterix reporter expression (red) was compared with immunostaining for *Osterix* protein (green) in tissue sections of 4-week-old femurs [tissue sections were counterstained with DAPI (blue)]. Comparison of expression was assessed in four different regions: **(a, b)** cortical bone, **(c, d)** trabecular bone, **(e, f)** growth plate cartilage, and **(g, h)** articular cartilage. *Osterix* reporter expression was highly expressed in osteoblasts lining the cortical **(a, white arrows)** and trabecular bone surfaces **(c)** and osteocytes embedded in bone tissue **(a)**. Immunostaining also revealed high levels of *Osterix* protein expression in osteoblasts lining cortical **(b, white arrows)** and trabecular bone surfaces **(d)**, but was difficult to detect in osteocytes **(b)**. **(e)** *Osterix* reporter expression was broadly expressed at low levels in growth plate chondrocytes with slightly higher levels of reporter expression present in maturing chondrocytes. **(f)** Immunostaining reveals *Osterix* protein was largely restricted to chondrocytes undergoing hypertrophy. At the end of the distal femur, *Osterix* reporter expression **(g)** and immunostaining for *Osterix* **(h)** correlate well in the articular cartilage as shown by overlapping signals in chondrocytes undergoing hypertrophy. (BM, bone marrow; CB, cortical bone; PS, primary spongiosa; SS, secondary spongiosa).

polyclonal antibody (A-13) was raised against this region of *Osterix* and therefore selectively detects the long protein isoform of *Osterix*. Unfortunately, many other antibodies against *Osterix* were tried, but did not work well in our hands. Alternatively, we decided to use the A-13 antibody on non-transgenic littermates and compare immunostaining (green fluorescence) to *Osterix* reporter expression (red fluorescence) (Fig. 7). Tissue sections were counterstained with DAPI (blue fluorescence). Four different regions of interest within the femur were compared; cortical bone (Fig. 7, compare A to B), trabecular bone (Fig. 7, compare C to D), the growth plate (Fig. 7, compare E to F), and the articular surface at the distal end of the femur (Fig. 7, compare G to H). In the cortical and trabecular bone regions, *Osterix* reporter expression appeared strongest in osteoblasts lining the bone surface (white arrows), but also had fairly high levels of expression in osteocytes within the bone tissue (Fig. 7 A and C). Consistent with *Osterix* reporter expression, immunostaining for *Osterix* was most intense in osteoblasts lining the cortical (white arrows) and trabecular bone surfaces, whereas noticeably less protein was detected in osteocytes (Fig. 7 B and D). As detailed earlier, *Osterix* reporter expression increased with age in maturing chondrocytes within the growth plate (Fig. 6). However, by four weeks of age and relative to osteoblasts and osteocytes, the *Osterix* reporter is expressed at lower levels in chondrocytes of the growth plate, with slightly higher levels being present in maturing chondrocytes (Fig. 7E). In contrast, immunostained *Osterix* protein was only detected in chondrocytes undergoing hypertrophy (Fig. 7E). Unlike the differences observed between reporter and immunostaining in the growth plate, Cherry expression correlated well with immunostaining in articular chondrocytes. In the knee joint, *Osterix* reporter expression

is absent from the most superficial zones of the articular surface in the distal femur, but appears in maturing chondrocytes further away from the articular surface (Fig. 7G, white arrows). In a similar manner, detection of *Osterix* protein was also present in maturing chondrocytes below the articular surface (Fig. 7).

While *Osterix* immunostaining largely correlated with *Osterix* reporter gene expression, some differences were observed. Possible reasons for these differences may relate to the fact that the reporter should reflect the expression of both transcriptional isoforms of *Osterix*, while the A-13 polyclonal antibody only recognized the long protein isoform. Additionally, post-transcriptional mechanisms that would regulate levels of *Osterix* protein would not be reflected in reporter gene expression.

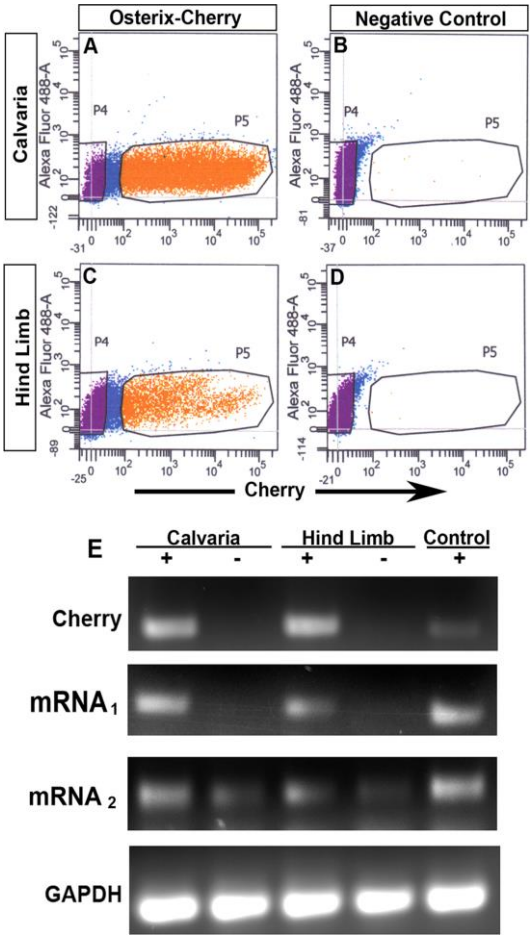

FIGURE 8: GENE EXPRESSION ANALYSIS OF OSTERIX MRNA ISOFORMS ON FACS ISOLATED PRIMARY CELLS

Primary cells were harvested from the calvaria and hind limb of Osterix reporter mice at postnatal day 5 and FACS isolated for gene expression studies. **(a–d**) FACS isolation of Osterix positive (P5-orange) and negative (P4-purple) cell populations from calvaria **(a)** and hind limb **(c)**. **(b, d)** Nontransgenic littermate controls are also shown. **(e)** Gene expression analysis was carried out for the Cherry reporter gene, both transcriptional isoforms of Osterix ($mRNA_1$ and $mRNA_2$) and GAPDH. Both transcriptional isoforms are detected in the Cherry positive cell fraction, while $mRNA_2$ was also weakly detected in the negative cell fraction.

To further compare expression of the *Osterix* reporter to endogenous *Osterix*, we also carried out RT-PCR on reporter positive and negative cell populations that were isolated by FACS from neonatal calvaria and long bones (Fig. 8, A-D). Approximately 50% of the cells digested out of the calvaria (Fig. 8A) and 12% of the cells digested from

long bones (Fig. 8C) were *Osterix* reporter positive. RT-PCR was carried out on the reporter (Cherry), the individual isoforms of *Osterix* ($mRNA_1$ and $mRNA_2$), and GAPDH (Fig. 8E). Amplification for the Cherry reporter confirmed that FACS dramatically enriched for the *Osterix* reporter positive and negative cell populations. Specific amplification for both alternative isoforms of *Osterix* revealed that $mRNA_1$ was exclusively expressed in the reporter positive cell population, while $mRNA_2$ could be detected in both cell fractions with higher levels being present in the reporter positive cell fraction.

While expression of the *Osterix* reporter was largely restricted to skeletal tissues, we also detected high levels of reporter expression for a transient period of time in the kidneys of newborn pups that gradually decreased by the time animals were weaned (Fig. 9). To further characterize renal *Osterix* reporter expression, kidney samples were collected from transgenic mice at E17.5 (Fig. 9A), P4 (Fig. 9B) and 3 weeks (Fig. 9C) of age and the intensity of fluorescent reporter expression was compared. Surprisingly, at E17.5 and 3 weeks, reporter expression was detectable, but very weak, while reporter expression at P4 was extremely high. We also examined *Osterix* reporter expression in 6 week and 11 week old transgenic animals, but no reporter expression was detected (data not shown). Further examination of *Osterix* reporter expression in tissue sections of P4 animals (Fig. 9, D, E, E', E'') revealed that reporter expression was present in the juxtamedullary nephrons, which are located in the cortex, but adjacent to the medulla (Fig. 9D). Within the juxtamedullary nephrons, *Osterix* reporter expression was detected at low levels in the proximal convoluted tubules and at higher levels in the thick descending limb of the loop of Henley (Fig. 9, E' and E").

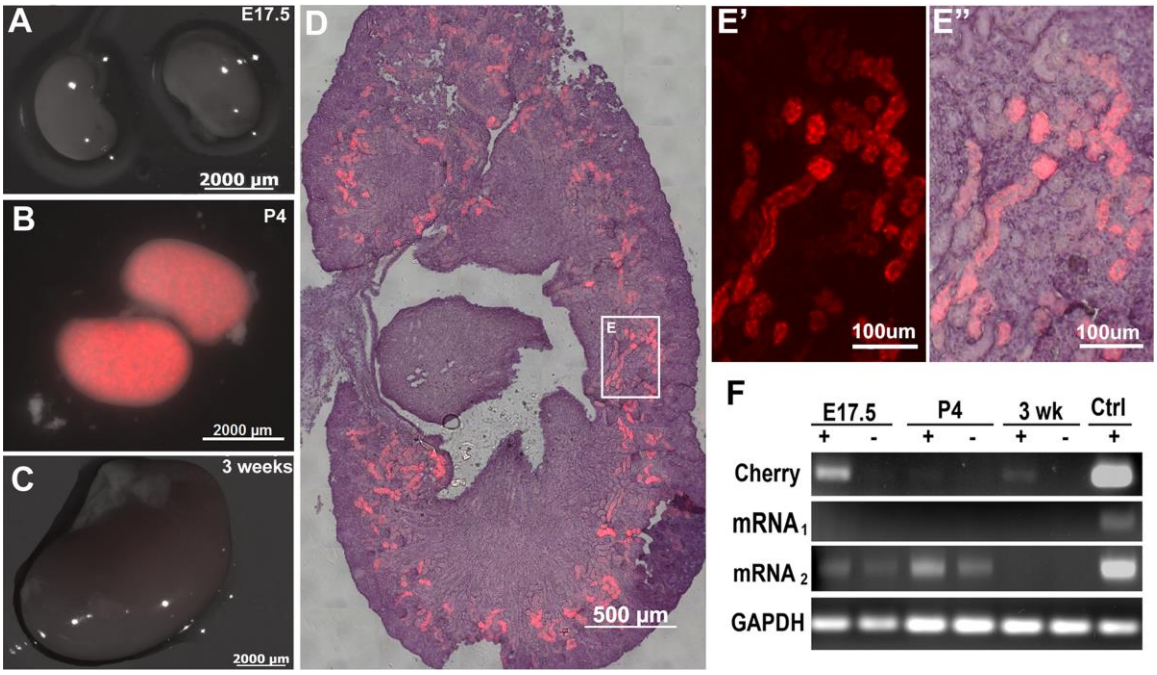

FIGURE 9: TRANSIENT *OSTERIX* REPORTER EXPRESSION IN THE KIDNEY

(a–c) Detection of *Osterix* reporter expression (red) in kidneys harvested from E17.5 **(a)**, post-natal day 4 (P4) **(b)**, and 3 week old **(c)** animals reveals the transient nature of reporter gene expression. **(d, e, e', e'')** Imaging of *Osterix* reporter expression in kidney tissue sections at P4. **(d)** Scanned image of a coronal section revealing *Osterix* reporter expression (red) in the juxtamedullary nephrons (purple-hematoxylin counterstaining). **(e', e'')** Reporter expression seen at high magnification from a region of interest shown in **(d)** revealing expression in the proximal convoluted tubule and the thick descending limb of loop of Henle. **(f)** Analyses of endogenous *Osterix* transcription showed that only mRNA2 was transiently detected in the kidney, while expression of mRNA1 was not detected.

To determine if *Osterix* is expressed transiently in the kidney, RT-PCR was carried out on transgenic positive and negative kidney samples at E17.5, P4, and 3 weeks of age (Fig. 9F). Interestingly, we were able to detect only one of the two isoforms in the kidney, $mRNA_{2.}$ Also, expression of the $mRNA_2$ isoform was transient, similar to that observed with our reporter gene. For reasons that remain unclear to us, we had a very difficult time detecting mRNA for the Cherry reporter in the kidney at P4, near the time point where we are able to visualize robust fluorescent expression.

In this study, we have described the transgene assembly and expression of an *Osterix*-Cherry fluorescent reporter mouse model. Characterization of reporter

expression suggests that the 39kb transgene largely retains many of the cis regulatory elements necessary for regulating *Osterix* gene expression in skeletal tissues from embryonic to adult ages. Consistent with *Osterix* having an essential role in osteoblast and chondrocyte development, *Osterix* reporter expression was largely restricted to both of these skeletal lineages. However, we have also noted transient reporter expression in the kidney that was particularly strong at neonatal ages. Given the timing of reporter expression in the kidney in relation to lactation, it is intriguing to speculate that perhaps *Osterix* may have a role in regulating mineral homeostasis during this period of active skeletal growth and development.

The transgenic reporter was designed to detect both transcriptional isoforms of *Osterix*. Other groups have reported on the existence and expression of both *Osterix* isoforms, however, there is disagreement with regard to which isoform may be the predominant form, if any. Milona et al. have reported that the shorter isoform ($mRNA_2$) is more highly expressed in skeletal cell types [41], while Nishio et al. provided evidence that the longer isoform ($mRNA_1$) predominates [2]. Our immunostaining studies, which have utilized an antibody that recognizes the long protein isoform of *Osterix,* clearly indicate that $mRNA_1$ is highly expressed in osteoblasts and hypertrophic chondrocytes. However, analyses of isoform specific transcripts by RT-PCR on FACS isolated cell populations indicate that both transcriptional isoforms are likely to be expressed in a relatively skeletal specific manner with perhaps $mRNA_2$ being expressed at significantly lower levels in non-skeletal cell types. It remains unclear if any functional differences exist between either protein isoform of *Osterix*.

One of the significant advantages of fluorescent protein reporter mice is that they provide investigators with the means to isolate and study intrinsically labeled cell populations. Work by us and others have generated a variety of different fluorescent reporter mice to study the osteoblast lineage [54, 64-66]. As a critical mediator of osteoblast commitment, *Osterix* has a very early and pivotal role within the osteoblast lineage. Supporting this thinking, the onset of *Osterix*-driven Cherry expression appeared earlier and in a broader cell population than *BSP* reporter expression during embryonic development. We also observed a low *Osterix* reporter expressing cell population in the bone marrow that was also *BSP* reporter negative, which may mark a very early osteoprogenitor required for supporting postnatal skeletal growth and bone maintenance. Therefore, *Osterix* reporter mice may provide us with a means to isolate and study the earliest cells of the osteoblast cell lineage, which still remain poorly understood.

CHAPTER V: DEFINING THE *OSTERIX*-CHERRY+ MESENCHYMAL PROGENITOR WITHIN THE BONE MARROW

ABSTRACT:

In this study, we have investigated the identity and biological properties of a bone marrow cell population retaining low *Osterix* reporter expression. Histological examination of reporter expression in bone tissue cross-sections revealed that bone marrow cells retaining low *Osterix* reporter expression were situated in proximity to endocortical bone surfaces and not uniformly distributed throughout the marrow. Immunostaining for the endothelial cell surface marker CD31 showed that approximately 40% of the *Osterix* reporter cells associated with the vascular sinusoids, but were not endothelial cells. Stromal cultures derived from *Osterix*-reporter mice showed that cherry+ cells flushed from the marrow attached to tissue culture plastic and expanded in culture. Furthermore, the *in vitro* differentiation of day 5 sorted *Osterix*-reporter cells along the osteoblast, chondrocyte, and adipocyte cell lineages provided evidence for their uncommitted multipotent skeletal potential. Additionally, during osteoblast differentiation, *Osterix* reporter expression dramatically increased supporting the belief that low *Osterix* reporter expression identifies an early skeletal progenitor. By FACS analysis, ~2% of the bone marrow retained cherry reporter fluorescence. Cell surface profiling on the bone marrow fraction indicated that the bone marrow cell population retaining *Osterix* reporter expression was very heterogeneous in nature being 60% positive for CD31, 60% positive for $CD11b_{low}$, and ~85-90% positive for $CD45_{low}$, CD44 and CD29. Surprisingly, few *Osterix* reporter expressing bone marrow cells were

positive for known mesenchymal cell markers Sca1, CD105, and CD140b, with the exception of CD90.2. However after culturing for five days, *Osterix*-Cherry cells adopted a mesenchymal cell profile by dramatically increasing in Sca1, CD105, and CD140b, but retained the hematopoietic cell surface markers CD45 and CD11b.

INTRODUCTION:

Our knowledge of bone marrow skeletal progenitor cells remains limited. Work by Friedenstein provided the first evidence that skeletal progenitor cells exist in the bone marrow and could be extracted and expanded in culture. This cell population was present at a low frequency inside the bone marrow, was adherent to tissue culture plastic, appeared fibroblast-like in cell morphology, retained skeletal potential and supported hematopoiesis [18]. Work by many other groups have substantiated Friedenstein's work [19, 20, 67] and cell culture remains the easiest way to enrich and expand for these skeletal progenitors. Because of their skeletal potential and accessibility through bone marrow aspiration, the application of these cells for therapeutic purposes has supported great research efforts to further define the identity and biological properties of these cells.

The *in vivo* identity of the cells which establish the hematopoietic environment in bone marrow has not been well defined [27]. In humans, CD146+ sub-endothelial cells have shown to be clonogenic upon transplantation, however, a similar marker in mice has not been determined[26, 27]. CD146+ sub-endothelial cells reside on the vascular sinusoidal network within the marrow. These cells produce large quantities of Angiopoietin-1 and are involved in the vascular remodeling of the sinusoidal network [27]. Other cell types have also been shown to have a role in the hematopoietic microenvironment. CAR cells, which are multipotent progenitor cells, also express cytokines necessary for the homing and maintenance of hematopoietic stem cells in the bone marrow and b-cell development, including CXCL12 and Stem Cell Factor (SCF)[24]. Another cell type within the hematopoietic niche is the Nestin+ reticular cell

[29, 68], which has been shown to be multipotent and which has also been shown to express *Osterix* [69].

Osterix is a zinc finger transcription factor, which functions as a key regulator of osteoblast differentiation [1, 2]. *Osterix* is selectively expressed in cells of the osteoblast lineage and has an essential function in osteoblast commitment and bone formation [1, 3]. While it is generally accepted that *Osterix* is expressed in early osteogenic precursors [3, 5-7], our understanding regarding the plasticity of these precursors for the osteoblast lineage relative to other cell lineages is lacking. However, recent fate mapping studies using *Osterix*-Cre mice have provided evidence that *Osterix* expression occurs in early uncommitted skeletal progenitor cells that contribute to a variety of cell lineages inside the bone marrow[70].

To better understand the early skeletal progenitor cell types retaining *Osterix* expression, we recently generated *Osterix*-Cherry reporter mice. Previous studies from our lab and others have used fluorescent reporter mice to aid in defining cells of the osteoblastic lineage [71, 72]. Inside the bone marrow of this animal model is a cell population retaining low *Osterix* reporter expression (LORE) that in many ways is morphologically reminiscent of a reticular cell population. Here we provide evidence that LORE cells represent a very early skeletal progenitor retaining multipotent skeletal potential.

RESULTS:

LORE CELLS ARE LOCATED NEAR THE ENDOSTEAL BONE SURFACE AND ARE ASSOCIATED WITH VASCULAR SINUSOIDS

The location of cells within the bone marrow stroma is proving to be a very important indicator of possible cellular function. Past characterization of *Osterix*-Cherry reporter mice showed strong reporter expression in mature osteoblasts and osteocytes[53]. Relative to the robust reporter expression in mature osteoblasts and osteocytes, we also noted a low *Osterix* reporter expressing cell population present within the bone marrow compartment that we have referred to as LORE cells.

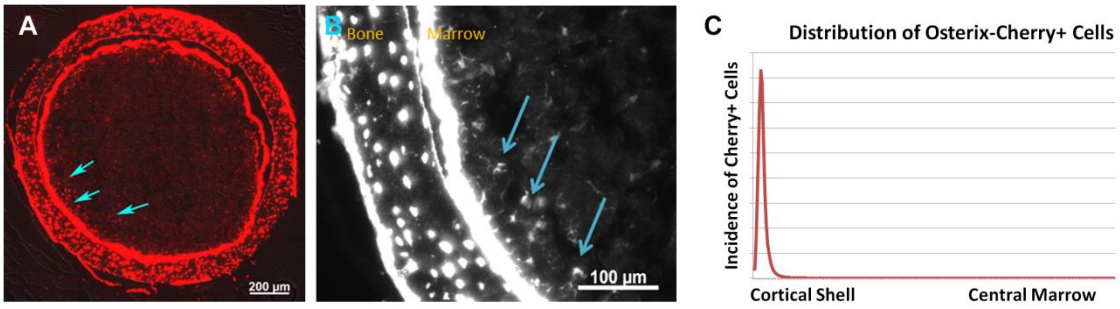

FIGURE 10: DISTRIBUTION OF *OSTERIX*-CHERRY+ CELLS IN THE BONE MARROW

(a) Cherry positive cells are seen in the periphery of the cortical bone, when the bone is cut in cross section (blue arrows) **(b)** High Magnification of the cortical bone, showing Cherry+ cells (blue arrows) appear predominantly near the endocortical surface with few positive cells appearing near the central region of the marrow. **(c)** Distribution pattern of *Osterix*-Cherry+ cells as assessed by Image J (representative graph); much of the Cherry+ cells appear adjacent to, or within the first 20% of the marrow radially, near the endocortical surface.

To better elucidate the location of these cells within the marrow, we sectioned long bones derived from *Osterix*-Cherry reporter mice in a longitudinal plane and in cross-section. As seen in the cross-section taken from the mid-diaphysis of a three week old femur, these cells seem to congregate near the endocortical surface (Fig 10 A, B high mag, blue arrows). There are very few LORE cells near the center of the marrow. The

LORE cells appear to be within the first few cell layers, under 100μm from the endocortical surface. This can also be seen if the bone is cut in a longitudinal section close to the endocortical surface (data not shown). Multiple sections were cut in the transverse plane and were analyzed to determine the distribution of the *Osterix*-Cherry+ cell in the marrow. The analysis showed that all of the *Osterix*-Cherry+ cells were located in a ring which included about 20% of the radius of the marrow space, near the endocortical surface (Fig 10C).

Many LORE cells morphologically appeared similar to bone marrow reticular cells, containing thin dendritic like processes. Along these lines, sub-endothelial perivascular stromal cells, which associate with the bone marrow vascular sinusoids have been shown to display skeletal potential [73]. Therefore, we carried out CD31 immunostaining to visualize the location of bone marrow endothelial cells to *Osterix*-Cherry+ cells. Immunostaining showed that a subpopulation of LORE cells were associated with the vascular sinusoidal network (Fig 11 A-C).

Based on our analysis of our immunostaining (and subsequent FACS) we knew that not all of the CD31+ cells were Cherry+, nor were all Cherry+ cells positive for CD31. However, we felt that it was likely that *Osterix*-Cherry cells were associating with CD31+ endothelial cells(Fig 11).

We also looked at Alkaline Phosphatase (ALP) staining using a set of reagents that was spectrally distinct from our Cherry reporter. ALP staining marked many of the *Osterix*-Cherry+ dendritic cells, especially those close to the endocortical surface (Fig 11 D-F).

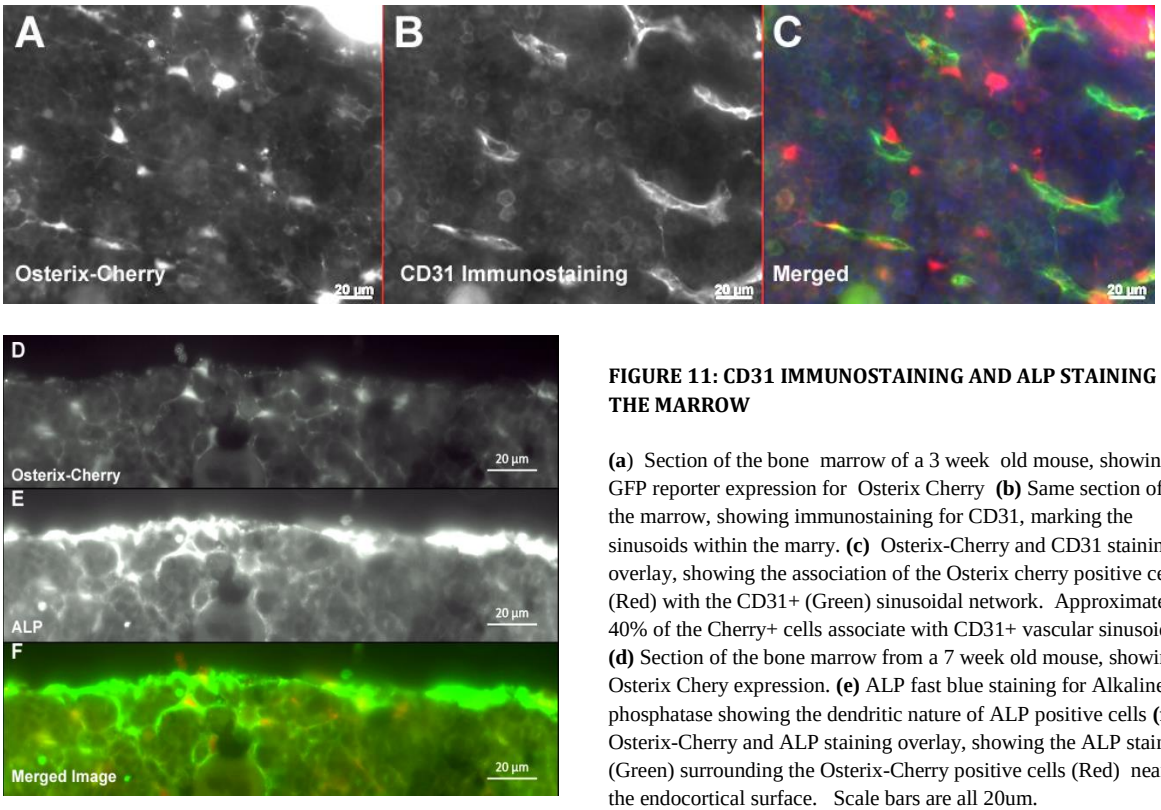

FIGURE 11: CD31 IMMUNOSTAINING AND ALP STAINING IN THE MARROW

(a) Section of the bone marrow of a 3 week old mouse, showing GFP reporter expression for Osterix Cherry **(b)** Same section of the marrow, showing immunostaining for CD31, marking the sinusoids within the marry. **(c)** Osterix-Cherry and CD31 staining overlay, showing the association of the Osterix cherry positive cells (Red) with the CD31+ (Green) sinusoidal network. Approximately 40% of the Cherry+ cells associate with CD31+ vascular sinusoids**.** **(d)** Section of the bone marrow from a 7 week old mouse, showing Osterix Chery expression. **(e)** ALP fast blue staining for Alkaline phosphatase showing the dendritic nature of ALP positive cells **(f)** Osterix-Cherry and ALP staining overlay, showing the ALP staining (Green) surrounding the Osterix-Cherry positive cells (Red) near the endocortical surface. Scale bars are all 20um.

EXAMINATION OF OSTERIX REPORTER EXPRESSION IN BONE MARROW STROMAL CULTURES

Given the detection of LORE cells inside the bone marrow, stromal cultures were carried out to determine if and how well LORE cells contributed to the overall adherent stromal cell population. By FACS roughly 1-2% of the total cell population from the flushed bone marrow retained *Osterix* reporter expression (Fig 12J). *Osterix* reporter labeled cells were imaged at progressive stages of culture during growth and osteogenic differentiation. In the heterogeneous environment of the stromal culture, we noted 24 hours after plating that a small subpopulation of fluorescent cells attached to tissue culture plastic, established a mesenchymal cell morphology, and were organized in small colonies of cells (Fig 12 A). For reasons that are not clear, some cell colonies persisted

in culture, while others did not. At days 3 and 4 of culture, reporter gene intensity decreased (Fig 12 A-D). However, after the addition of osteogenic inducing agents at day 7, the intensity of *Osterix* reporter expression noticeably increased (Fig 12 compare E to F). By day 14 of culture, strong *Osterix* reporter expression can be detected in colonies defining putative regions of mature osteoblast differentiation (Fig 12F). By day 21, *Osterix* reporter expression was even brighter and correlated with areas of mineralization detected by von Kossa (Fig 12 compare G to H).

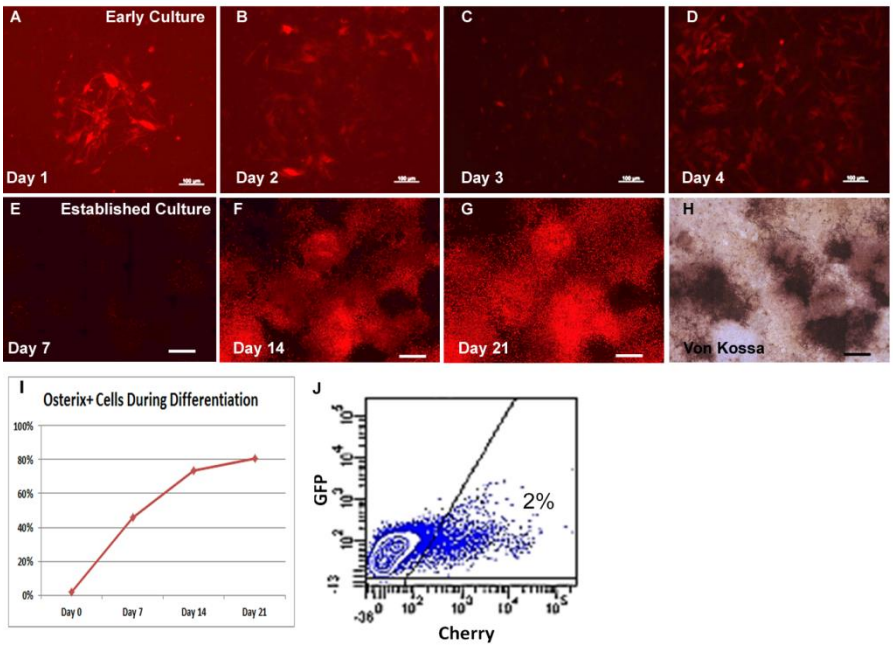

FIGURE 12: *OSTERIX*-CHERRY EXPRESSION CHANGES DURING DIFFERENTIATION

(a-d) Early culture progression from 24 hours after plating (Day 1) to Day 4. *Osterix* Cherry expression gets more diffuse and weaker at the early stages of culture, though the number of cells which are *Osterix*-Cherry+ continues to increase. The weakening trend reverses at Day 5, at which point the cells increase in intensity through the culture period **(e-i)** Established culture progression up through Day 21 of osteogenic differentiation. *Osterix* Cherry expression continues to increase as the culture progresses **(e-g)** Days 7, 14 and 21 of culture showing weaker *Osterix*-Cherry colonies spread throughout the plate, which increase at Day 14 and further increase at Day 21. Exposure times are consistent **(h)** Von Kossa staining of a Day 21 culture, showing that areas of mineralization correlate with areas of strongest *Osterix*-Cherry expression **(i)** FACS analysis shows the percentage of stromal cells isolated from the marrow are Cherry + up through Day 21 of the culture period **(j)** FACS analysis showing the percentage of *Osterix*-Cherry+ cells in the flushed bone marrow

We also quantified the percentage of cells retaining cherry fluorescence protein by FACS. At day 0, approximately 2% of the cells isolated from the bone marrow are

Cherry+. This increased substantially by day 4, with approximately 30% of the cells becoming Cherry+ (data not shown). By day 7, close to 50% of these cells are positive for *Osterix*-Cherry and by day 21, when the culture is actively mineralizing, approximately 80% of the total cells in the culture are Cherry+ (Fig 12I).

LORE CELLS RETAIN MULTIPOTENT SKELETAL POTENTIAL

To further characterize the stromal cell population retaining *Osterix* reporter expression, we carried out *in vitro* differentiation studies. For these studies, the *Osterix* reporter labeled cell population was FACS sorted from day 5 stromal cultures, replated in culture, and differentiated along the osteoblast, adipocyte, and chondrocyte cell lineages. *In vitro* differentiation was assessed by using histological staining to detect mineral deposition (Fig. 13C), von Kossa), lipid vesicle formation (Fig. 13G, Oil Red-O), and proteoglycan production (Fig.13K, Alcian blue). Gene expression analyses were also carried out on days 0, 5 and 8 (osteoblast and adipocyte cultures) or days 0, 7 and 14 (chondrocyte cultures) to assess differentiation (Fig.13 D, H, L).

Not surprisingly, sorted *Osterix* reporter labeled cells efficiently differentiated into bone. During osteoblast differentiation, *Osterix* reporter expression substantially increased (Fig.13A and previously shown in Fig12), mineralization was visible under DIC optics (Fig 13B) and by von Kossa staining (Fig 13C). During osteoblast differentiation, mRNA levels of *Bone Sialoprotein* (*BSP*), *Osteocalcin*, and *Dentin Matrix Protein* (*DMP1*) also dramatically increased.

Sorted *Osterix* labeled cells also retained the capacity to differentiate into adipocytes. During adipocyte differentiation, reporter expression decreased substantially

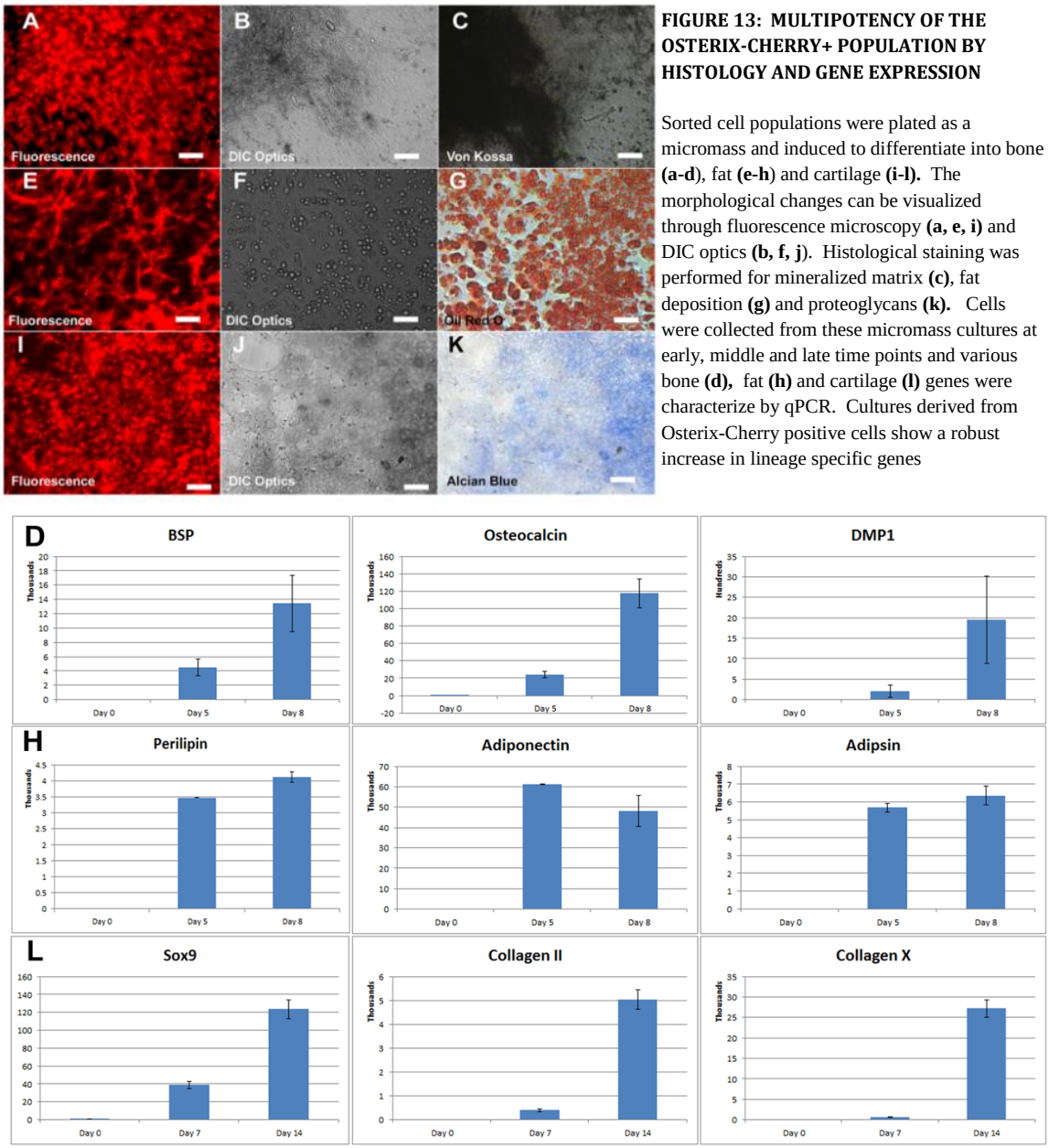

FIGURE 13: MULTIPOTENCY OF THE OSTERIX-CHERRY+ POPULATION BY HISTOLOGY AND GENE EXPRESSION

Sorted cell populations were plated as a micromass and induced to differentiate into bone **(a-d**), fat **(e-h**) and cartilage **(i-l).** The morphological changes can be visualized through fluorescence microscopy **(a, e, i)** and DIC optics **(b, f, j**). Histological staining was performed for mineralized matrix **(c)**, fat deposition **(g)** and proteoglycans **(k).** Cells were collected from these micromass cultures at early, middle and late time points and various bone **(d),** fat **(h)** and cartilage **(l)** genes were characterize by qPCR. Cultures derived from Osterix-Cherry positive cells show a robust increase in lineage specific genes

in cells that developed large lipid vesicles, while mesenchymal cells located around forming adipocytes maintained *Osterix* reporter expression. Changes in cell morphology and large lipid vesicles were observed under DIC optics (Fig 13F) and Oil Red O staining for lipids was also detected throughout the culture (Fig 13G). Gene expression analyses also showed that the adipocyte gene markers *Adiponectin*, *Adipsin* and *Perilipin* were all substantially up-regulated during differentiation (Fig 13H).

Sorted *Osterix*-Cherry+ cells also retained the ability to differentiate into chondrocytes. During chondrocyte differentiation, cells maintained their *Osterix* reporter expression, but the intensity of the reporter was less compared to levels of expression during osteoblast differentiation (Fig 13I). Under DIC optics, mesenchymal cells formed condensations within the micromass (Fig 13J) and proteoglycan expression could be detected by staining with Alcian Blue (Fig 13K). Gene expression analyses of chondrocyte formation showed up-regulation of *Sox9*, *Collagen type 2 alpha 1*, and *Collagen type 10 alpha 1* (Fig 13L).

Taken together, these *in vitro* studies provide evidence that *Osterix* reporter labeled cells from the bone marrow contribute to a stromal cell population that retains multipotent skeletal potential.

CELL SURFACE PROFILING AND GENE EXPRESSION FROM LORE CELLS REVEALS THEIR HETEROGENEITY

To further understand the identity and homogeneity of the bone marrow cell population retaining *Osterix* reporter expression, cell surface profiling was carried out on cells directly flushed from the bone marrow and after 5 days in culture. As previously mentioned, between 1-2% of the total bone marrow fraction retained *Osterix* reporter expression (Fig 12 J), though this can be divided into two parts based on the intensity of the cherry expression (Fig 14, Gating Control). A variety of cell surface markers were used including hematopoietic (CD45 and CD11b), endothelial (CD31), and mesenchymal (CD44, Sca1, CD29, CD105, CD90.2 and CD140b).

When profiled directly from the bone marrow, three populations of cells were elucidated: a cherry negative fraction (blue), a cherry low population (green) and a cherry high population (red). All cell populations have high levels of CD45 (~75-95%), CD44 (>85%) and C29 (>85%). Cherry positive cells from both groups show higher levels of CD11b (~60%) than the negative fraction (~30%). The cherry high population has significantly higher levels of CD31 (~85%) than either the negative (~35%) or the low (~50%), likely due to the association of those cells with the vascular sinusoidal network. All populations have low levels of Sca1 (<10%), CD105 (<10%) and CD140b (<5%). Of interest is CD90, which is considered to be an MSC marker; approximately 50% of the cherry positive cells were positive for CD90, whereas less than 5% of the cherry low or negative cells were positive for CD90 (Fig 14).

After culturing for 5 days, the cell surface profile of the *Osterix*-Cherry population significantly changed (Fig 15). Minimal CD31 expression was detected and mesenchymal markers Sca1, CD105, and CD140b all markedly increased in the cherry positive population. Interestingly, hematopoietic cell surface markers CD45 and CD11b still persisted, in many cases at higher levels than initially detected directly from the marrow. CD105 and CD140b are detected at very low levels in the negative; however these markers are now expressed in 40% and 70% of the cherry positive cells, respectively. CD90 expression in the cherry positive population is lost in culture.

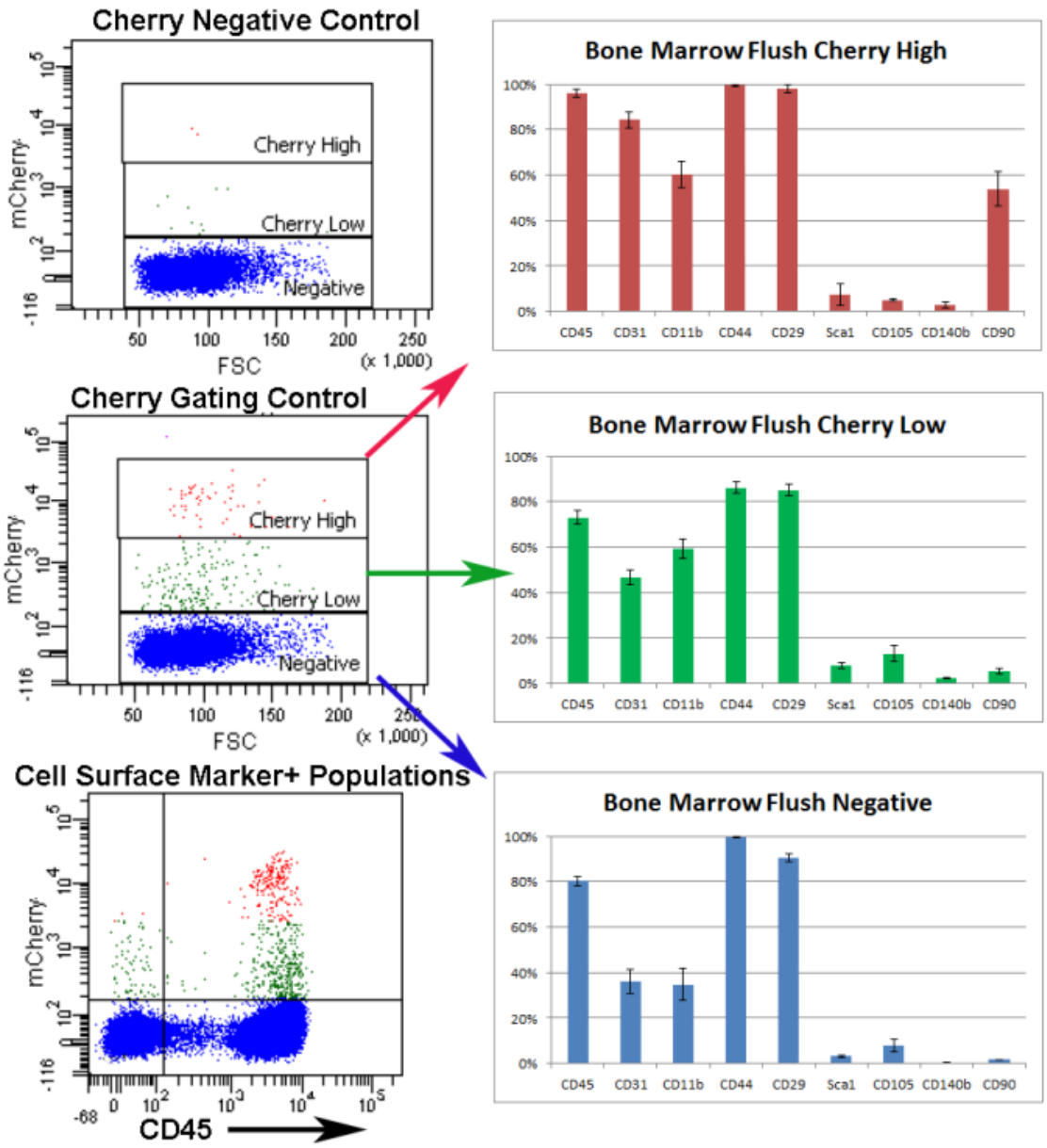

FIGURE 14 : CELL SURFACE PROFILING FROM THE BONE MARROW

Cells flushed from the marrow of 3-week old mice (n=3) were gated based on cherry expression into 3 groups: negative (Blue), cherry low (Green) and cherry high(Red). Each group was analyzed for a variety of cell surface markers including CD45, CD31, CD11b, CD44, CD29, Sca1, CD105, CD140b and CD90. The cell surface marker+ populations graph shows a typical plot, in this case, CD45, indicating where each population falls per quadrant. Populations were analyzed and the percentage of cells in each group which was positive for the marker was graphed.

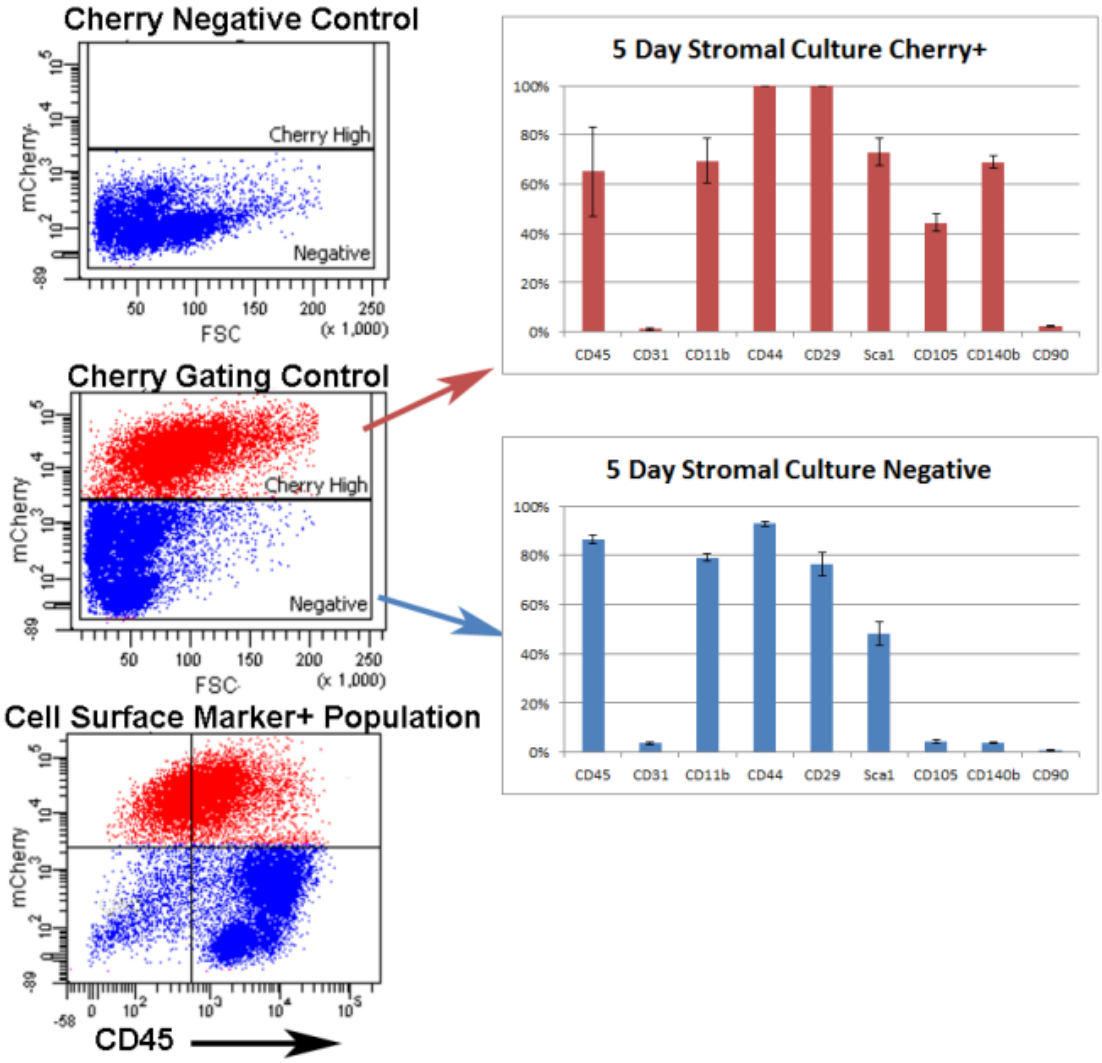

FIGURE 15 : CELL SURFACE PROFILE OF CULTURED BONE MARROW CELLS

Cells flushed from the marrow of 3-week old mice (n=3) were individually cultured for 5 days, then enzymatically digested and subjected to FACS sorting. Cells were gated based on cherry expression into 2 groups: negative (blue) and cherry high (red). Each group was analyzed for a variety of cell surface markers including CD45, CD31, CD11b, CD44, CD29, Sca1, CD105, CD140b and CD90. The cell surface marker+ populations graph shows a typical plot, in this case, CD45, indicating where each population falls per quadrant. Populations were analyzed and the percentage of cells in each group which was positive for the marker was graphed.

Culturing the bone marrow drastically changes the cell surface profile. The most dramatic change is the loss of the lowest expressing cherry positive population. The expression of cherry in the cultured cells is much more uniform than that seen directly from the marrow. After culture, cherry positive cells lose CD90 and CD31, but gain mesenchymal markers like Sca1, CD140b and CD105. Clearly, the environmental

differences between the bone marrow and those seen during cell culture result in notable changes in the cell surface phenotype.

To try to further determine the identity of the *Osterix*-Cherry positive cell, we also examined the expression of Stem Cell Factor (SCF) and CXCL12 in the our *Osterix*-Cherry sorted fraction directly from the bone marrow, as these markers have been shown to be upregulated in the sub-endothelial cells in the niche that are multipotent. *Osterix* was increased about 30-40 fold in the cherry positive population compared to the cherry negative population (confirming our sort efficiency and that our reporter model is accurately marking cells expressing *Osterix* (data not shown)). CxCl12 and Stem Cell Factor were both modestly upregulated in the sorted cherry positive population compared to the cherry negative (Fig 16).

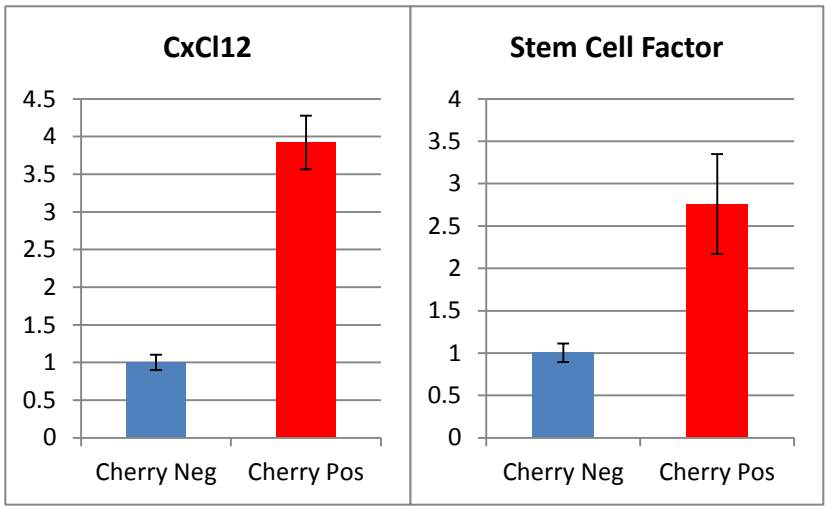

FIGURE 16: UPREGULATION OF CXCL12 AND STEM CELL FACTOR IN SORTED CHERRY POSITIVE CELLS FROM THE MARROW

Cells directly from the marrow were sorted, RNA was extracted and cDNA was made. qPCR was performed for CXCL12 and Stem Cell Factor. There is modest upregulation of both in the cherry positive population as compared to the cherry negative.

DISCUSSION:

In this study, we have investigated a novel bone marrow cell population retaining low *Osterix* reporter expression (LORE). Given the functional role of *Osterix* and the location of LORE cells in proximity to endocortical bone surfaces, a reasonable assumption is that LORE cells may represent an early osteoprogenitor cell type. In agreement with this thinking, staining for alkaline phosphatase, an early gene marker of osteogenesis co-localized with many LORE cells. However, further characterization of the LORE cell population implicated that at least a subpopulation may be comparable to bone marrow mesenchymal stem cells (BMSCs) or the multipotent perivascular stromal cell. First, immunostaining in tissue section showed that ~43% of LORE cells associated with the vascular sinusoids similar to other multipotent perivascular stromal cell types. Second, gene expression levels for perivascular gene markers SCF and Cxcl12 were all up-regulated in the *Osterix*-Cherry+ cell fraction compared to the negative cell fraction. Third, a subpopulation of *Osterix*-Cherry+ cells were adherent to tissue culture plastic and grew in colonies as one would expect from BMSCs [19, 20]. Finally, *in vitro* differentiation of sorted *Osterix*-Cherry cells provided evidence for their skeletal multipotency.

At the same time, cell surface profiling indicates that the LORE cell population is likely to be heterogeneous. *Osterix* reporter labeling seems to favor higher expression of CD11b and cells which express high levels of cherry also express high levels of CD90.

As these cells are cultured, their cell surface profile changes. The Cherry+ population loses expression of CD31, and gains expression of more mesenchymal

markers, like CD44, CD29, Sca1, CD105 and CD140b [67, 74], with culture. Traditionally, CD45 and CD11b are not considered to be expressed in a mesenchymal population; however, our data shows that both markers remain high after 5 days in culture. We are currently studying the CD45+ and the CD11b+ population to try to determine why these markers seem to be maintained in our population. Ooi, et al. suggested that BMSCs originally start out as CD45+ and then lose that expression over time. [75, 76] This is similar to what we are seeing with our Cherry+ cell population.

The bone marrow is a very heterogeneous environment. Teasing out various cell populations, even with the tools available to us, is difficult. In this study, we have identified a small population expressing *Osterix* in the bone marrow that associates with the vascular sinusoids and is ALP+. This *Osterix*-Cherry+ cell adheres to tissue culture plastic and is multipotent. However, there are subpopulations within this small population which make further characterization difficult. Multiple cell types reside on or near the vascular sinusoidal network. These cells often display similar properties to our *Osterix*-Cherry+ population. The *Osterix*-Cherry reporter allows us to pull apart some of these populations based on intensity and proximity to the endocortical surface, but we have yet to fully characterize all of the subpopulations that are reporter positive that we see within the marrow.

CHAPTER VI: OVERVIEW AND FUTURE DIRECTIONS:

Fluorescent reporter animal models are valuable tools to investigate biological processes. To learn more about osteoblast biology, in this thesis, we have presented work on the generation and characterization of *Osterix*-Cherry reporter mice. While the utility of this animal model may have broad applications within the field of skeletal research, our studies have been primarily focused in two areas. First, characterizing reporter expression in correlation to the endogenous *Osterix* gene expression and secondly, scrutinizing the identity of cell types retaining reporter expression with a particular interest on bone marrow skeletal progenitor cells. Our *Osterix* reporter mice have allowed us to tease out some of the intricacies of the *Osterix* gene and its regulation.

OSTERIX EXPRESSION IS NOT EXCLUSIVE TO THE OSTEOBLAST LINEAGE

The importance of *Osterix* for osteoblast differentiation is well established [1, 7, 44, 63, 77, 78], thus we anticipated reporter expression would be largely exclusive to cells of the osteoblast lineage. In agreement with previous studies, *Osterix* reporter expression was highly and selectively expressed in cells of the osteoblast lineage with strong reporter expression being present in mature osteoblasts and osteocytes. However, our studies also revealed that *Osterix* is also expressed in maturing chondrocytes. Interestingly, *Osterix* reporter expression progressively increased in growth plate chondrocytes with age. Consistent with these observations, recent work has validated an essential role for *Osterix* in chondrocyte differentiation [62].

In addition to the growth plate, during early postnatal life, we also detected very robust, but transient *Osterix* reporter expression in the collecting ducts of the kidneys. The timing of expression in newborn animals seemed to coincide with the onset of suckling. Thus, while a role for *Osterix* in the kidney remains to be determined, we speculate that *Osterix* may be involved in the regulation of calcium-phosphate reabsorption during this very active phase of skeletal growth.

LOW *OSTERIX* REPORTER EXPRESSION MARKS A BONE MARROW CELL POPULATION

While *Osterix* reporter expression was robustly detected in mature osteoblasts and osteocytes, we also noted cells present within the bone marrow that retained low levels of reporter expression. Careful examination of *Osterix* reporter expression by sectioning bone tissue in cross-section revealed that low *Osterix* reporter cells were located in proximity to endocortical bone surfaces. Compared to previously generated osteoblast reporter mouse models, including *Bone Sialoprotein* –Topaz and *Collagen 1a1 3.6*–Cyan, which had little to no expression in any bone marrow cell population, the detection of *Osterix* reporter expression in a bone marrow cell population was novel.

Given the early role for *Osterix* in osteoblast differentiation and the proximity of these cells adjacent to the bone surface, we hypothesized that this cell population was an early osteoprogenitor cell population. One of the benefits we found with this mouse is that we have a fluorescent population within the marrow that can be FACS isolated, allowing for careful analysis of this specific stromal population, even though it makes up

a very small percentage (1-3%) of the marrow. Thus, our work from that point forward sought to characterize this cell population.

OSTERIX REPORTER EXPRESSION STROMAL CELLS DISPLAY MESENCHYMAL MULTIPOTENCY

Stromal cultures derived from *Osterix* reporter mice revealed that cells taken from the bone marrow containing *Osterix* reporter expression directly contributed to an adherent cell population. This was recently confirmed by FACS isolation of *Osterix* reporter positive cells directly from the bone marrow and their contribution to colony formation in co-cultures. Interestingly, *in vitro* differentiation studies implicate that the *Osterix* reporter expressing cell population does retain multipotent properties, being able to differentiate into osteoblasts, adipocytes, and chondrocytes, *in vitro*. These findings were somewhat surprising because it is well established that functionally *Osterix* has an important role in osteoblast commitment [7, 11, 41, 63]. However, consistent with our studies, recent fate mapping studies demonstrated how embryonic progenitors labeled by *Osterix*-Cre and *Osterix*-CreERT2 mice traced into a variety of cell types within the bone marrow including adipocyte, perineural, vascular smooth muscle, and stromal in addition to the osteoblast lineage[70]. Thus, low and early *Osterix* reporter expression potentially identifies a cell population of osteoprogenitor cells that are not fully committed to the osteoblast lineage and can contribute to other cell lineages.

Our studies also suggest that the post-transcriptional regulation of *Osterix* is likely to be critically important for osteoblast differentiation. In this regard, some recent studies have started to elucidate at least some of the post-transcriptional mechanisms

which regulate *Osterix* function[77]. BMP2/ Smad signaling can act indirectly on *Osterix* through Runx2 and Dlx5. Both of these pathways, along with the activation of the MAPK signaling cascade will enhance the phosphorylation and thus enhance the expression of *Osterix*, as does Igf1 and the Unfolded Protein Response[79-81]. TNFa and p53 can repress the expression of *Osterix* by preventing its phosphorylation [3, 82]. Also, various other mechanisms, like DNA methylation and microRNAs allow for epigenetic control of *Osterix* expression [83, 84]. Further studies have shown the NO66 represses phosphorylated *Osterix* activity and NFATc enhances the activity of phosphorylated *Osterix* [85-87].

CLINICAL RELEVANCE OF *OSTERIX*:

Osterix has recently been implicated in a variety of skeletal diseases. Originally, based on mouse studies, deficiencies in *Osterix* were thought to be lethal in humans as well, but some recent studies by Lapunzina et al have identified a Single Nucleotide Polymorphism (SNP) in an Egyptian Osteogenesis Imperfecta (OI) patient, producing a truncated *Osterix* protein[88]. Osteogenesis Imperfecta has long been associated with mutations in *Collagen*, not *Osterix*, so this mutation shows another potential causative agent for OI. Genome Wide Association Studies (GWAS) have shown that SNPs in *Osterix* are strongly correlated with adult lumbar spine BMD and increased BMD in females with childhood obesity [89, 90]. Taken together, these studies show a clear significance for *Osterix* in bone health[77].

In order to study how *Osterix* is involved in bone disease, we could modulate various factors: one could examine how the disease process or a potential treatment effects cells of all stages of the osteogenic lineage based on our Cherry reporter. We have the potential to be able to regulate *Osterix in vivo* and *in vitro* using small molecules– looking at how agonists and antagonists of certain pathways change the expression of the reporter.

AN UNEXPECTED CELL SURFACE PROFILE FOR *OSTERIX* REPORTER EXPRESSING BONE MARROW CELLS

To more clearly define the bone marrow cell population retaining low *Osterix* reporter expression, we carried out cell surface profiling directly from the bone marrow and from day 5 stromal cultures. While the cell surface profile of osteoprogenitor cells has not been well defined, because of their mesenchymal-like multipotency, we speculated they might have a cell surface profile similar to previously reported bone marrow stromal cell populations. Surprisingly, characterization directly from the bone marrow revealed a more complex profile that included cell surface markers commonly associated with the hematopoietic and endothelial cell lineages including CD45+, CD11b+, and CD31+. The potential significance of hematopoietic cell marker expression on the *Osterix* reporter expressing cell population remains unclear. Perhaps it is a signature correlated with cell-cell communication occurring in the bone marrow. Additionally, three known mesenchymal cell surface markers (CD44, CD29, and CD90) were up-regulated in the *Osterix* reporter population while other mesenchymal markers like Sca1 and CD105 and CD140b were scarcely present.

Interestingly, transition into a cell culture environment resulted in a significant alteration in cell surface profile more consistent with what has been previously reported for mesenchymal stem cells. After 5 days in culture, *Osterix* reporter cells were Sca1+, CD105+ and CD140b+ in addition to having very high levels of CD44 and CD29. Surprisingly, they also retained CD45+ and CD11b+ surface markers; however the staining intensity for these hematopoietic markers was lower than that of the negative fraction. The alteration in cell surface profiling from the bone marrow environment to the tissue culture environment may reflect a combination of possibilities. First, different environments resulted in substantial changes in cell profiles. The *in vivo* bone marrow environment is substantially more complex and likely to have broader diversity, whereas the tissue culture environment is more uniform, thus similar cells will have a common response and possibly alter their cell surface phenotype in the same manner. Additionally, during the transition from the bone marrow environment to the cell culture environment, a substantial selection process takes place resulting in the presence and expansion of certain cell types over others.

The expression of cell surface markers more consistent with the myeloid lineage (CD11b, CD115, and F4/80) on *Osterix* reporter cells is currently an area we are actively investigating. It remains unclear if these are macrophages that have engulfed dead osteoblasts and have acquired cherry fluorescence through phagocytosis or if the gene expression of these cell surface markers remains promiscuous and crosses over into the osteoblast lineage.

A second possibility is that a subpopulation of *Osterix* reporter expressing cells are fibrocytes. Fibrocytes are mesenchymal progenitors that exhibit characteristics of

hematopoietic stem cells, monocytes and fibroblasts [91]. These cells have a very similar cell surface marker profile to what we are seeing in our reporter positive cells, especially from the bone marrow. Based on the markers we tested, both our reporter positive cells and fibrocytes are CD45+, CD11b+ and CD29+ [91, 92]. Future experiments will try to tease out the identity of the *Osterix* reporter expressing cells in the marrow.

CELLULAR HETEROGENEITY AND THE BIOLOGICAL COMPLEXITY OF THE BONE MARROW ENVIRONMENT

The bone marrow is a complex and heterogeneous environment. There are multiple cell types and niches within the marrow itself which each have their own unique biology and characteristics. Studies from our lab have shown that most cell types which contribute to the structure of the stroma, maintain their niche and location within the marrow[70]. Clearly, there is evidence that given the functional role of *Osterix* and the location of *Osterix*–Cherry+ cells in proximity to endocortical bone surfaces, a reasonable assumption is that these cells may represent an early osteoprogenitor cell type, but it is also possible that progenitor cells may be reacting to signals within their local environment such that cells which are closer to the endosteal surface take on different characteristics then when they are in the center of the marrow. Our *Osterix*-Cherry+ cells are likely representing at least two subpopulations, based on reporter intensity, cell surface profiling, immunostaining results and proximity to the bone surface. Further studies will be necessary to elucidate the identity of each subpopulation of *Osterix*-Cherry+ cells and to characterize their distinct roles in the marrow environment and why *Osterix* expression is needed for these cell types.

APPENDIX

License Agreement from Wiley

JOHN WILEY AND SONS LICENSE TERMS AND CONDITIONS

Nov 26, 2013

This is a License Agreement between Peter Maye ("You") and John Wiley and Sons ("John Wiley and Sons") provided by Copyright Clearance Center ("CCC"). The license consists of your order details, the terms and conditions provided by John Wiley and Sons, and the payment terms and conditions.

All payments must be made in full to CCC. For payment instructions, please see information listed at the bottom of this form.

License Number	3276641038460
License date	Nov 26, 2013
Licensed content publisher	John Wiley and Sons
Licensed content publication	genesis
Licensed content title	Generation and characterization of Osterix-Cherry reporter mice
Licensed copyright line	Copyright © 2013 Wiley Periodicals, Inc.
Licensed content author	Sara Strecker,Yu Fu,Yaling Liu,Peter Maye
Licensed content date	Dec 19, 2012
Start page	246
End page	258
Type of use	Dissertation/Thesis
Requestor type	Author of this Wiley article
Format	Print and electronic
Portion	Full article
Will you be translating?	No
Total	0.00 USD
Terms and Conditions	

TERMS AND CONDITIONS

This copyrighted material is owned by or exclusively licensed to John Wiley & Sons, Inc. or one of its group companies (each a "Wiley Company") or a society for whom a Wiley Company has exclusive publishing rights in relation to a particular journal (collectively "WILEY"). By clicking "accept" in connection with completing this licensing transaction, you agree that the following terms and conditions apply to this transaction (along with the billing and payment terms and conditions established by the Copyright Clearance Center Inc., ("CCC's Billing and Payment terms and conditions"), at the time that you opened your RightsLink account (these are available at any time at http://myaccount.copyright.com).

Terms and Conditions

1. The materials you have requested permission to reproduce (the "Materials") are protected by copyright.

2.You are hereby granted a personal, non-exclusive, non-sublicensable, non-transferable, worldwide, limited license to reproduce the Materials for the purpose specified in the licensing process. This license is for a one-time use only with a maximum distribution equal to the number that you identified in the licensing process. Any form of republication granted by this license must be completed within two years of the date of the grant of this license (although copies prepared before may be distributed thereafter). The Materials shall not be used in any other manner or for any other purpose. Permission is granted subject to an appropriate acknowledgement given to the author, title of the material/book/journal and the publisher. You shall also duplicate the copyright notice that appears in the Wiley publication in your use of the Material. Permission is also granted on the understanding that nowhere in the text is a previously published source acknowledged for all or part of this Material. Any third party material is expressly excluded from this permission.

3. With respect to the Materials, all rights are reserved. Except as expressly granted by the terms of the license, no part of the Materials may be copied, modified, adapted (except for minor reformatting required by the new Publication), translated, reproduced, transferred or distributed, in any form or by any means, and no derivative works may be made based on the Materials without the prior permission of the respective copyright owner. You may not alter, remove or suppress in any manner any copyright, trademark or other notices displayed by the Materials. You may not license, rent, sell, loan, lease, pledge, offer as security, transfer or assign the Materials, or any of the rights granted to you hereunder to any other person.

4. The Materials and all of the intellectual property rights therein shall at all times remain the exclusive property of John Wiley & Sons Inc or one of its related companies (WILEY) or their respective licensors, and your interest therein is only that of having possession of and the right to reproduce the Materials pursuant to Section 2 herein during the continuance of this Agreement. You agree that you own no right, title or interest in or to the Materials or any of the intellectual property rights therein. You shall have no rights hereunder other than the license as provided for above in Section 2. No right, license or interest to any trademark, trade name, service mark or other branding ("Marks") of WILEY or its licensors is granted hereunder, and you agree that you shall not assert any such right, license or interest with respect thereto.

5. NEITHER WILEY NOR ITS LICENSORS MAKES ANY WARRANTY OR REPRESENTATION OF ANY KIND TO YOU OR ANY THIRD PARTY, EXPRESS, IMPLIED OR STATUTORY, WITH RESPECT TO THE MATERIALS OR THE ACCURACY OF ANY INFORMATION CONTAINED IN THE MATERIALS, INCLUDING, WITHOUT LIMITATION, ANY IMPLIED WARRANTY OF MERCHANTABILITY, ACCURACY, SATISFACTORY QUALITY, FITNESS FOR A PARTICULAR PURPOSE, USABILITY, INTEGRATION OR NON-INFRINGEMENT AND ALL SUCH WARRANTIES ARE HEREBY EXCLUDED BY WILEY AND ITS

LICENSORS AND WAIVED BY YOU.

6. WILEY shall have the right to terminate this Agreement immediately upon breach of this Agreement by you.

7. You shall indemnify, defend and hold harmless WILEY, its Licensors and their respective directors, officers, agents and employees, from and against any actual or threatened claims, demands, causes of action or proceedings arising from any breach of this Agreement by you.

8. IN NO EVENT SHALL WILEY OR ITS LICENSORS BE LIABLE TO YOU OR ANY OTHER PARTY OR ANY OTHER PERSON OR ENTITY FOR ANY SPECIAL, CONSEQUENTIAL, INCIDENTAL, INDIRECT, EXEMPLARY OR PUNITIVE DAMAGES, HOWEVER CAUSED, ARISING OUT OF OR IN CONNECTION WITH THE DOWNLOADING, PROVISIONING, VIEWING OR USE OF THE MATERIALS REGARDLESS OF THE FORM OF ACTION, WHETHER FOR BREACH OF CONTRACT, BREACH OF WARRANTY, TORT, NEGLIGENCE, INFRINGEMENT OR OTHERWISE (INCLUDING, WITHOUT LIMITATION, DAMAGES BASED ON LOSS OF PROFITS, DATA, FILES, USE, BUSINESS OPPORTUNITY OR CLAIMS OF THIRD PARTIES), AND WHETHER OR NOT THE PARTY HAS BEEN ADVISED OF THE POSSIBILITY OF SUCH DAMAGES. THIS LIMITATION SHALL APPLY NOTWITHSTANDING ANY FAILURE OF ESSENTIAL PURPOSE OF ANY LIMITED REMEDY PROVIDED HEREIN.

9. Should any provision of this Agreement be held by a court of competent jurisdiction to be illegal, invalid, or unenforceable, that provision shall be deemed amended to achieve as nearly as possible the same economic effect as the original provision, and the legality, validity and enforceability of the remaining provisions of this Agreement shall not be affected or impaired thereby.

10. The failure of either party to enforce any term or condition of this Agreement shall not constitute a waiver of either party's right to enforce each and every term and condition of this Agreement. No breach under this agreement shall be deemed waived or excused by either party unless such waiver or consent is in writing signed by the party granting such waiver or consent. The waiver by or consent of a party to a breach of any provision of this Agreement shall not operate or be construed as a waiver of or consent to any other or subsequent breach by such other party.

11. This Agreement may not be assigned (including by operation of law or otherwise) by you without WILEY's prior written consent.

12. Any fee required for this permission shall be non-refundable after thirty (30) days from receipt

13. These terms and conditions together with CCC's Billing and Payment terms and conditions (which are incorporated herein) form the entire agreement between you and WILEY concerning this licensing transaction and (in the absence of fraud) supersedes all prior agreements and representations of the parties, oral or written. This Agreement may not be amended except in writing signed by both parties. This Agreement shall be binding upon and inure to the benefit of the parties' successors, legal representatives, and authorized assigns.

14. In the event of any conflict between your obligations established by these terms and conditions

and those established by CCC's Billing and Payment terms and conditions, these terms and conditions shall prevail.

15. WILEY expressly reserves all rights not specifically granted in the combination of (i) the license details provided by you and accepted in the course of this licensing transaction, (ii) these terms and conditions and (iii) CCC's Billing and Payment terms and conditions.

16. This Agreement will be void if the Type of Use, Format, Circulation, or Requestor Type was misrepresented during the licensing process.

17. This Agreement shall be governed by and construed in accordance with the laws of the State of New York, USA, without regards to such state's conflict of law rules. Any legal action, suit or proceeding arising out of or relating to these Terms and Conditions or the breach thereof shall be instituted in a court of competent jurisdiction in New York County in the State of New York in the United States of America and each party hereby consents and submits to the personal jurisdiction of such court, waives any objection to venue in such court and consents to service of process by registered or certified mail, return receipt requested, at the last known address of such party.

Wiley Open Access Terms and Conditions

Wiley publishes Open Access articles in both its Wiley Open Access Journals program [http://www.wileyopenaccess.com/view/index.html] and as Online Open articles in its subscription journals. The majority of Wiley Open Access Journals have adopted the Creative Commons Attribution License (CC BY) which permits the unrestricted use, distribution, reproduction, adaptation and commercial exploitation of the article in any medium. No permission is required to use the article in this way provided that the article is properly cited and other license terms are observed. A small number of Wiley Open Access journals have retained the Creative Commons Attribution Non Commercial License (CC BY-NC), which permits use, distribution and reproduction in any medium, provided the original work is properly cited and is not used for commercial purposes.

Online Open articles - Authors selecting Online Open are, unless particular exceptions apply, offered a choice of Creative Commons licenses. They may therefore select from the CC BY, the CC BY-NC and the Attribution-NoDerivatives (CC BY-NC-ND). The CC BY-NC-ND is more restrictive than the CC BY-NC as it does not permit adaptations or modifications without rights holder consent.

Wiley Open Access articles are protected by copyright and are posted to repositories and websites in accordance with the terms of the applicable Creative Commons license referenced on the article. At the time of deposit, Wiley Open Access articles include all changes made during peer review, copyediting, and publishing. Repositories and websites that host the article are responsible for incorporating any publisher-supplied amendments or retractions issued subsequently.
Wiley Open Access articles are also available without charge on Wiley's publishing platform, **Wiley Online Library** or any successor sites.

Conditions applicable to all Wiley Open Access articles:

- The authors' moral rights must not be compromised. These rights include the right of "paternity" (also known as "attribution" - the right for the author to be identified as such) and "integrity" (the right for the author not to have the work altered in such a way that the author's reputation or integrity may be damaged).

- Where content in the article is identified as belonging to a third party, it is the obligation of the user to ensure that any reuse complies with the copyright policies of the owner of that content.

- If article content is copied, downloaded or otherwise reused for research and other purposes as permitted, a link to the appropriate bibliographic citation (authors, journal, article title, volume, issue, page numbers, DOI and the link to the definitive published version on Wiley Online Library) should be maintained. Copyright notices and disclaimers must not be deleted.
    - Creative Commons licenses are copyright licenses and do not confer any other rights, including but not limited to trademark or patent rights.

- Any translations, for which a prior translation agreement with Wiley has not been agreed, must prominently display the statement: "This is an unofficial translation of an article that appeared in a Wiley publication. The publisher has not endorsed this translation."

Conditions applicable to non-commercial licenses (CC BY-NC and CC BY-NC-ND)

For non-commercial and non-promotional purposes individual non-commercial users may access, download, copy, display and redistribute to colleagues Wiley Open Access articles. In addition, articles adopting the CC BY-NC may be adapted, translated, and text- and data-mined subject to the conditions above.

Use by commercial "for-profit" organizations

Use of non-commercial Wiley Open Access articles for commercial, promotional, or marketing purposes requires further explicit permission from Wiley and will be subject to a fee. Commercial purposes include:

- Copying or downloading of articles, or linking to such articles for further redistribution, sale or licensing;

- Copying, downloading or posting by a site or service that incorporates advertising with such content;

- The inclusion or incorporation of article content in other works or services (other than normal quotations with an appropriate citation) that is then available for sale or licensing, for a fee (for example, a compilation produced for marketing purposes, inclusion in a sales pack)

- Use of article content (other than normal quotations with appropriate citation) by for-profit organizations for promotional purposes
- Linking to article content in e-mails redistributed for promotional, marketing or educational purposes;
- Use for the purposes of monetary reward by means of sale, resale, license, loan, transfer or other form of commercial exploitation such as marketing products
- Print reprints of Wiley Open Access articles can be purchased from: corporatesales@wiley.com

The modification or adaptation for any purpose of an article referencing the CC BY-NC-ND License requires consent which can be requested from RightsLink@wiley.com .

Other Terms and Conditions:

BY CLICKING ON THE "I AGREE..." BOX, YOU ACKNOWLEDGE THAT YOU HAVE READ AND FULLY UNDERSTAND EACH OF THE SECTIONS OF AND PROVISIONS SET FORTH IN THIS AGREEMENT AND THAT YOU ARE IN AGREEMENT WITH AND ARE WILLING TO ACCEPT ALL OF YOUR OBLIGATIONS AS SET FORTH IN THIS AGREEMENT.

v1.8

If you would like to pay for this license now, please remit this license along with your payment made payable to "COPYRIGHT CLEARANCE CENTER" otherwise you will be invoiced within 48 hours of the license date. Payment should be in the form of a check or money order referencing your account number and this invoice number RLNK501168489. Once you receive your invoice for this order, you may pay your invoice by credit card. Please follow instructions provided at that time.

Make Payment To:
Copyright Clearance Center
Dept 001
P.O. Box 843006
Boston, MA 02284-3006

For suggestions or comments regarding this order, contact RightsLink Customer Support: customercare@copyright.com or +1-877-622-5543 (toll free in the US) or +1-978-646-2777.

Gratis licenses (referencing $0 in the Total field) are free. Please retain this printable

license for your reference. No payment is required.

WORKS CITED

1. Nakashima, K., et al., *The novel zinc finger-containing transcription factor osterix is required for osteoblast differentiation and bone formation.* Cell, 2002. **108**(1): p. 17-29.

2. Nishio, Y., et al., *Runx2-mediated regulation of the zinc finger Osterix/Sp7 gene.* Gene, 2006. **372**: p. 62-70.

3. Zhou, X., et al., *Multiple functions of Osterix are required for bone growth and homeostasis in postnatal mice.* Proc Natl Acad Sci U S A. **107**(29): p. 12919-24.

4. Services, U.S.D.o.H.a.H., *Bone Health and Osteoporosis: A Report of the Surgeon General*, 2004, U.S. Department of Health and Human Services: Washington, D.C.

5. Nakashima, K. and B. de Crombrugghe, *Transcriptional mechanisms in osteoblast differentiation and bone formation.* Trends Genet, 2003. **19**(8): p. 458-66.

6. Mackie, E.J., et al., *Endochondral ossification: how cartilage is converted into bone in the developing skeleton.* Int J Biochem Cell Biol, 2008. **40**(1): p. 46-62.

7. Baek, W.Y., et al., *Positive regulation of adult bone formation by osteoblast-specific transcription factor osterix.* J Bone Miner Res, 2009. **24**(6): p. 1055-65.

8. Ugolotti, U., et al., *Peripheral arteriography with a new nonionic agent: comparison of iomeprol with iopamidol.* European journal of radiology, 1994. **18 Suppl 1**: p. S77-82.

9. Chavarria, G.E., et al., *Initial evaluation of the antitumour activity of KGP94, a functionalized benzophenone thiosemicarbazone inhibitor of cathepsin L.* European journal of medicinal chemistry, 2012. **58**: p. 568-72.

10. Khurana, J.S., E.F. McCarthy, and P.J. Zhang, *Essentials in bone and soft-tissue pathology*, New York: Springer. ix, 225 p.

11. Long, F., *Building strong bones: molecular regulation of the osteoblast lineage.* Nat Rev Mol Cell Biol. **13**(1): p. 27-38.

12. Mankani, M.H., et al., *Pedicled bone flap formation using transplanted bone marrow stromal cells.* Archives of surgery, 2001. **136**(3): p. 263-70.

13. Mackie, E.J., L. Tatarczuch, and M. Mirams, *The skeleton: a multi-functional complex organ: the growth plate chondrocyte and endochondral ossification.* J Endocrinol. **211**(2): p. 109-21.

14. Monaco, A.P., Z. Larin, and H. Lehrach, *Construction of yeast artificial chromosome libraries by pulsed-field gel electrophoresis.* Molecular biotechnology, 1994. **1**(3): p. 241-9.

15. Arthur, A., A. Zannettino, and S. Gronthos, *The therapeutic applications of multipotential mesenchymal/stromal stem cells in skeletal tissue repair.* J Cell Physiol, 2009. **218**(2): p. 237-45.

16. Pawelczyk, E., et al., *In vivo transfer of intracellular labels from locally implanted bone marrow stromal cells to resident tissue macrophages.* PloS one, 2009. **4**(8): p. e6712.

17. Friedenstein, A.J., S. Piatetzky, II, and K.V. Petrakova, *Osteogenesis in transplants of bone marrow cells.* J Embryol Exp Morphol, 1966. **16**(3): p. 381-90.

18. Friedenstein, A.Y. and K.S. Lalykina, *Lymphoid cell populations are competent systems for induced osteogenesis.* Calcif Tissue Res, 1970: p. Suppl:105-6.

19. Krebsbach, P.H., et al., *Bone marrow stromal cells: characterization and clinical application.* Crit Rev Oral Biol Med, 1999. **10**(2): p. 165-81.

20. Bianco, P., et al., *Bone marrow stromal stem cells: nature, biology, and potential applications.* Stem cells, 2001. **19**(3): p. 180-92.

21. Dexter, T.M., et al., *The regulation of hemopoietic cell development by the stromal cell environment and diffusible regulatory molecules.* Prog Clin Biol Res, 1984. **148**: p. 13-33.

22. Nagasawa, T., Y. Omatsu, and T. Sugiyama, *Control of hematopoietic stem cells by the bone marrow stromal niche: the role of reticular cells.* Trends Immunol. **32**(7): p. 315-20.

23. Suire, C., et al., *Isolation of the stromal-vascular fraction of mouse bone marrow markedly enhances the yield of clonogenic stromal progenitors.* Blood. **119**(11): p. e86-95.

24. Omatsu, Y., et al., *The essential functions of adipo-osteogenic progenitors as the hematopoietic stem and progenitor cell niche.* Immunity. **33**(3): p. 387-99.

25. Sugiyama, T. and T. Nagasawa, *Bone marrow niches for hematopoietic stem cells and immune cells.* Inflamm Allergy Drug Targets. **11**(3): p. 201-6.

26. Bianco, P., B. Sacchetti, and M. Riminucci, *Osteoprogenitors and the hematopoietic microenvironment.* Best Pract Res Clin Haematol. **24**(1): p. 37-47.

27. Sacchetti, B., et al., *Self-renewing osteoprogenitors in bone marrow sinusoids can organize a hematopoietic microenvironment.* Cell, 2007. **131**(2): p. 324-36.

28. Churchman, S.M., et al., *Native CD271(+) multipotential stromal cells (MSCs) have a transcript profile indicative of multiple fates with prominent osteogenic and Wnt pathway signalling activity.* Arthritis Rheum.

29. Mendez-Ferrer, S., et al., *Mesenchymal and haematopoietic stem cells form a unique bone marrow niche.* Nature. **466**(7308): p. 829-34.

30. Larin, Z., et al., *Fluorescence in situ hybridisation of multiple probes on a single microscope slide.* Nucleic acids research, 1994. **22**(18): p. 3689-92.

31. Menegazzi, P., et al., *Identification and characterization of three calmodulin binding sites of the skeletal muscle ryanodine receptor.* Biochemistry, 1994. **33**(31): p. 9078-84.

32. Newman, P.J., et al., *PECAM-1 (CD31) cloning and relation to adhesion molecules of the immunoglobulin gene superfamily.* Science, 1990. **247**(4947): p. 1219-22.

33. Treves, S., et al., *Alteration of intracellular Ca2+ transients in COS-7 cells transfected with the cDNA encoding skeletal-muscle ryanodine receptor carrying a mutation associated with malignant hyperthermia.* The Biochemical journal, 1994. **301 (Pt 3)**: p. 661-5.

34. Saeed, H., et al., *Mouse embryonic fibroblasts (MEF) exhibit a similar but not identical phenotype to bone marrow stromal stem cells (BMSC).* Stem Cell Rev. **8**(2): p. 318-28.

35. Haack, T.B., et al., *Homozygous missense mutation in BOLA3 causes multiple mitochondrial dysfunctions syndrome in two siblings.* Journal of inherited metabolic disease, 2012.

36. Larin, D.I., et al., *[Study of the transmembrane organization of the C-terminal domain of the alpha subunit of Na+,K+-ATPase using polyclonal antibodies to its perimembrane fragments]*. Bioorganicheskaia khimiia, 1994. **20**(8-9): p. 833-41.

37. Long, F. and D.M. Ornitz, *Development of the endochondral skeleton.* Cold Spring Harbor perspectives in biology, 2013. **5**(1): p. a008334.

38. Eames, B.F. and J.A. Helms, *Conserved molecular program regulating cranial and appendicular skeletogenesis.* Dev Dyn, 2004. **231**(1): p. 4-13.

39. Monaco, A.P. and Z. Larin, *YACs, BACs, PACs and MACs: artificial chromosomes as research tools.* Trends in biotechnology, 1994. **12**(7): p. 280-6.

40. Zelzer, E. and B.R. Olsen, *The genetic basis for skeletal diseases.* Nature, 2003. **423**(6937): p. 343-8.

41. Milona, M.A., J.E. Gough, and A.J. Edgar, *Expression of alternatively spliced isoforms of human Sp7 in osteoblast-like cells.* BMC Genomics, 2003. **4**: p. 43.

42. Gao, Y., et al., *Molecular cloning, structure, expression, and chromosomal localization of the human Osterix (SP7) gene.* Gene, 2004. **341**: p. 101-10.

43. Oh, J.H., et al., *Chondrocyte-specific ablation of Osterix leads to impaired endochondral ossification.* Biochem Biophys Res Commun. **418**(4): p. 634-40.

44. Baek, W.Y., B. de Crombrugghe, and J.E. Kim, *Postnatally induced inactivation of Osterix in osteoblasts results in the reduction of bone formation and maintenance.* Bone. **46**(4): p. 920-8.

45. Zimmer, M., *GFP: from jellyfish to the Nobel prize and beyond.* Chem Soc Rev, 2009. **38**(10): p. 2823-32.

46. Fu, Y. and P. Maye, *Engineering BAC reporter gene constructs for mouse transgenesis.* Methods Mol Biol. **693**: p. 163-79.

47. Kotzamanis, G. and C. Huxley, *Recombining overlapping BACs into a single larger BAC.* BMC Biotechnol, 2004. **4**: p. 1.

48. Gong, S., L. Kus, and N. Heintz, *Rapid bacterial artificial chromosome modification for large-scale mouse transgenesis.* Nat Protoc. **5**(10): p. 1678-96.

49. Court, D.L., et al., *Mini-lambda: a tractable system for chromosome and BAC engineering.* Gene, 2003. **315**: p. 63-9.

50. Liu, P., N.A. Jenkins, and N.G. Copeland, *A highly efficient recombineering-based method for generating conditional knockout mutations.* Genome Res, 2003. **13**(3): p. 476-84.

51. Gong, S., et al., *Highly efficient modification of bacterial artificial chromosomes (BACs) using novel shuttle vectors containing the R6Kgamma origin of replication.* Genome Res, 2002. **12**(12): p. 1992-8.

52. Wang, J., et al., *An improved recombineering approach by adding RecA to lambda Red recombination.* Mol Biotechnol, 2006. **32**(1): p. 43-53.

53. Strecker, S., et al., *Generation and characterization of osterix-cherry reporter mice.* Genesis, 2012.

54. Maye, P., et al., *A BAC-bacterial recombination method to generate physically linked multiple gene reporter DNA constructs.* BMC Biotechnol, 2009. **9**: p. 20.

55. Schneider, C.A., W.S. Rasband, and K.W. Eliceiri, *NIH Image to ImageJ: 25 years of image analysis.* Nature methods, 2012. **9**(7): p. 671-5.

56. Villa, M.M., et al., *Visualizing osteogenesis in vivo within a cell-scaffold construct for bone tissue engineering using two-photon microscopy.* Tissue engineering. Part C, Methods, 2013. **19**(11): p. 839-49.

57. Lo Celso, C. and D.T. Scadden, *The haematopoietic stem cell niche at a glance.* Journal of cell science, 2011. **124**(Pt 21): p. 3529-35.

58. Hall, B.K. and T. Miyake, *All for one and one for all: condensations and the initiation of skeletal development.* Bioessays, 2000. **22**(2): p. 138-47.

59. Mackie, E.J., L. Tatarczuch, and M. Mirams, *The skeleton: a multi-functional complex organ: the growth plate chondrocyte and endochondral ossification.* J Endocrinol, 2011. **211**(2): p. 109-21.

60. Ornitz, D.M. and P.J. Marie, *FGF signaling pathways in endochondral and intramembranous bone development and human genetic disease.* Genes Dev, 2002. **16**(12): p. 1446-65.

61. Gordon, J.A., et al., *Bone sialoprotein expression enhances osteoblast differentiation and matrix mineralization in vitro.* Bone, 2007. **41**(3): p. 462-73.

62. Oh, J.H., et al., *Chondrocyte-specific ablation of Osterix leads to impaired endochondral ossification.* Biochem Biophys Res Commun, 2012. **418**(4): p. 634-40.

63. Zhou, X., et al., *Multiple functions of Osterix are required for bone growth and homeostasis in postnatal mice.* Proc Natl Acad Sci U S A, 2010. **107**(29): p. 12919-24.

64. Kalajzic, I., et al., *Dentin matrix protein 1 expression during osteoblastic differentiation, generation of an osteocyte GFP-transgene.* Bone, 2004. **35**(1): p. 74-82.

65. Kalajzic, I., et al., *Use of type I collagen green fluorescent protein transgenes to identify subpopulations of cells at different stages of the osteoblast lineage.* J Bone Miner Res, 2002. **17**(1): p. 15-25.

66. Kalajzic, Z., et al., *Directing the expression of a green fluorescent protein transgene in differentiated osteoblasts: comparison between rat type I collagen and rat osteocalcin promoters.* Bone, 2002. **31**(6): p. 654-60.

67. Meirelles Lda, S. and N.B. Nardi, *Murine marrow-derived mesenchymal stem cell: isolation, in vitro expansion, and characterization.* British journal of haematology, 2003. **123**(4): p. 702-11.

68. Kollet, O., et al., *Regulatory cross talks of bone cells, hematopoietic stem cells and the nervous system maintain hematopoiesis.* Inflamm Allergy Drug Targets. **11**(3): p. 170-80.

69. Greenbaum, A., et al., *CXCL12 in early mesenchymal progenitors is required for haematopoietic stem-cell maintenance.* Nature, 2013. **495**(7440): p. 227-30.

70. Liu, Y., et al., *Osterix-cre labeled progenitor cells contribute to the formation and maintenance of the bone marrow stroma.* PloS one, 2013. **8**(8): p. e71318.

71. Kalajzic, I., et al., *Use of type I collagen green fluorescent protein transgenes to identify subpopulations of cells at different stages of the osteoblast lineage.* Journal of bone and mineral research : the official journal of the American Society for Bone and Mineral Research, 2002. **17**(1): p. 15-25.

72. Balic, A. and M. Mina, *Identification of secretory odontoblasts using DMP1-GFP transgenic mice.* Bone, 2011. **48**(4): p. 927-37.

73. Taylor, S.S., Z. Larin, and C.T. Smith, *Addition of functional human telomeres to YACs.* Human molecular genetics, 1994. **3**(8): p. 1383-6.

74. Koide, Y., et al., *Two distinct stem cell lineages in murine bone marrow.* Stem cells, 2007. **25**(5): p. 1213-21.

75. Deschaseaux, F., et al., *Direct selection of human bone marrow mesenchymal stem cells using an anti-CD49a antibody reveals their CD45med,low phenotype.* British journal of haematology, 2003. **122**(3): p. 506-17.

76. Ooi, Y.Y., R. Ramasamy, and S. Vidyadaran, *Mouse bone marrow mesenchymal stem cells acquire CD45-CD106+ immunophenotype only at later passages.* The Medical journal of Malaysia, 2008. **63 Suppl A**: p. 65-6.

77. Sinha, K.M. and X. Zhou, *Genetic and molecular control of osterix in skeletal formation.* J Cell Biochem, 2013. **114**(5): p. 975-84.

78. Tai, G., et al., *Use of green fluorescent fusion protein to track activation of the transcription factor osterix during early osteoblast differentiation.* Biochem Biophys Res Commun, 2005. **333**(4): p. 1116-22.

79. Huang, W., et al., *Signaling and transcriptional regulation in osteoblast commitment and differentiation.* Frontiers in bioscience : a journal and virtual library, 2007. **12**: p. 3068-92.

80. Celil, A.B., J.O. Hollinger, and P.G. Campbell, *Osx transcriptional regulation is mediated by additional pathways to BMP2/Smad signaling.* Journal of cellular biochemistry, 2005. **95**(3): p. 518-28.

81. Tohmonda, T., et al., *The IRE1alpha-XBP1 pathway is essential for osteoblast differentiation through promoting transcription of Osterix.* EMBO reports, 2011. **12**(5): p. 451-7.

82. Liu, H. and B. Li, *p53 control of bone remodeling.* Journal of cellular biochemistry, 2010. **111**(3): p. 529-34.

83. Chen, Q., et al., *Identification and characterization of microRNAs controlled by the osteoblast-specific transcription factor Osterix.* PLoS One, 2013. **8**(3): p. e58104.

84. Baglìo, S.R., et al., *MicroRNA expression profiling of human bone marrow mesenchymal stem cells during osteogenic differentiation reveals Osterix regulation by miR-31.* Gene, 2013. **527**(1): p. 321-31.

85. Sinha, K.M., et al., *Regulation of the osteoblast-specific transcription factor Osterix by NO66, a Jumonji family histone demethylase.* EMBO J. **29**(1): p. 68-79.

86. Sinha, K.M., et al., *Osterix and NO66 histone demethylase control the chromatin architecture of Osterix target genes during osteoblast differentiation.* J Bone Miner Res, 2013.

87. Koga, T., et al., *NFAT and Osterix cooperatively regulate bone formation.* Nature medicine, 2005. **11**(8): p. 880-5.

88. Lapunzina, P., et al., *Identification of a frameshift mutation in Osterix in a patient with recessive osteogenesis imperfecta.* Am J Hum Genet, 2010. **87**(1): p. 110-4.

89. Zhao, J., et al., *BMD-associated variation at the Osterix locus is correlated with childhood obesity in females.* Obesity (Silver Spring), 2011. **19**(6): p. 1311-4.

90. Timpson, N.J., et al., *Common variants in the region around Osterix are associated with bone mineral density and growth in childhood.* Hum Mol Genet, 2009. **18**(8): p. 1510-7.

91. Bellini, A. and S. Mattoli, *The role of the fibrocyte, a bone marrow-derived mesenchymal progenitor, in reactive and reparative fibroses.* Laboratory investigation; a journal of technical methods and pathology, 2007. **87**(9): p. 858-70.

92. Reilkoff, R.A., R. Bucala, and E.L. Herzog, *Fibrocytes: emerging effector cells in chronic inflammation.* Nature reviews. Immunology, 2011. **11**(6): p. 427-35.